Quantitative Analysis of Substantia Nigra Pars Reticulata Activity During a Visually Guided Saccade Task

ARI HANDEL AND PAUL W. GLIMCHER
Center for Neural Science, New York University, New York, New York 10003

Handel, Ari and Paul W. Glimcher. Quantitative analysis of substantia nigra pars reticulata activity during a visually guided saccade task. *J. Neurophysiol.* 82: 3458–3475, 1999. Several lines of evidence suggest that the pars reticulata subdivision of the substantia nigra (SNr) plays a role in the generation of saccadic eye movements. However, the responses of SNr neurons during saccades have not been examined with the same level of quantitative detail as the responses of neurons in other key saccadic areas. For this report, we examined the firing rates of 72 SNr neurons while awake-behaving primates correctly performed an average of 136 trials of a visually guided delayed saccade task. On each trial, the location of the visual target was chosen randomly from a grid spanning 40° of horizontal and vertical visual angle. We measured the firing rates of each neuron during five intervals on every trial: a baseline interval, a fixation interval, a visual interval, a movement interval, and a reward interval. We found four distinct classes of SNr neurons. Two classes of neurons had firing rates that decreased during delayed saccade trials. The firing rates of *discrete pausers* decreased after the onset of a contralateral target and/or before the onset of a saccade that would align gaze with that target. The firing rates of *universal pausers* decreased after fixation on all trials and remained below baseline until the delivery of reinforcement. We also found two classes of SNr neurons with firing rates that increased during delayed saccade trials. The firing rates of *bursters* increased after the onset of a contralateral target and/or before the onset of a saccade aligning gaze with that target. The firing rates of *pause-bursters* increased after the onset of a contralateral target but decreased after the illumination of an ipsilateral target. Our quantification of the response profiles of SNr neurons yielded three novel findings. First, we found that some SNr neurons generate saccade-related increases in activity. Second, we found that, for nearly all SNr neurons, the relationship between firing rate and horizontal and vertical saccade amplitude could be well described by a planar surface within the range of movements we sampled. Finally we found that for most SNr neurons, saccade-related modulations in activity were highly variable on a trial-by-trial basis.

INTRODUCTION

For most of the nearly 350 years since the basal ganglia first were distinguished by Willis (1664, 1978), their role in motor control has been the subject of much speculation but little certainty (cf. Marsden 1980). In the late 1970s and early 1980s, a possible oculomotor role for the basal ganglia was raised by anatomic data demonstrating a dense, inhibitory, GABAergic projection from a major output nucleus of the basal ganglia, the substantia nigra pars reticulata (SNr), to the intermediate layers of the superior colliculus (SC) (cf. Beckstead 1981; DiChiara et al. 1979; Hopkins and Niessen 1976; Huerta and Harting 1984; Jayaraman et al. 1977; Ma 1989; Vincent et al. 1978; Wurtz and Albano 1980), a major saccadic control center (for reviews of the SC and saccadic control, see Sparks 1986; Sparks and Mays 1990; Wurtz and Albano 1980). To demonstrate a physiological role for this pathway and thereby link basal ganglia studies to one of the simplest and best-studied motor systems, Hikosaka and Wurtz recorded from hundreds of SNr neurons in monkeys trained to make saccades in response to visual stimuli (Hikosaka and Wurtz 1983a–d).

Hikosaka and Wurtz found a population of neurons in the lateral portion of the SNr that tonically generated action potentials at 50–100 spikes/s but decreased this rate of activity after the presentation of saccadic targets or before the generation of saccades in oculomotor tasks (Hikosaka and Wurtz 1983a; for similar results in cat, see Joseph and Boussaoud 1985). Closely related pharmacological experiments indicated that GABAergic manipulations of both the superior colliculus and the SNr profoundly affected the properties of saccadic eye movements (Hikosaka and Wurtz 1985a,b; for cat, see Boussaoud and Joseph 1985). Based on these data, Hikosaka and Wurtz proposed that the SNr may be an important component of the oculomotor system that functions by tonically inhibiting the superior colliculus and then releasing that inhibition before saccades (Hikosaka and Wurtz 1989).

This hypothesis has been extended by the observation that the central region of the caudate, a principal afferent source of the SNr (Hikosaka et al. 1993; Parent et al. 1984; Szabo 1970), also carries visual and saccade-related signals (Hikosaka et al. 1989a–c). The central region of the caudate is itself innervated by multiple cortical areas, including the frontal eye fields (FEF) (Kunzle and Akert 1977), an area that carries well-studied visual and saccade-related signals (cf. Bruce and Goldberg 1985; Segraves and Goldberg 1987). Although the FEF is only one possible source of caudate visual and saccade-related signals (cf. Alexander et al. 1986; Hikosaka et al. 1989a), a broadly accepted hypothesis has emerged (cf. Alexander et al. 1986; Hikosaka and Wurtz 1989; Kandel et al. 1991; Leigh and Zee 1991; Wurtz and Hikosaka 1986) that the SNr specifically, and the oculomotor basal ganglia in general, lies primarily within a FEF-SC circuit. However, a more detailed comparison of the response properties of neurons in the FEF, SNr, and SC, which would provide a more rigorous test of the hypothesis that the SNr relays saccade-related signals from the FEF (via the caudate) to the SC, is not possible until the SNr has been examined with the same degree of quantitative detail as the FEF and SC (for detailed studies of the FEF, see Bruce and Goldberg 1985; Bruce et al. 1985; Segraves and Goldberg

The costs of publication of this article were defrayed in part by the payment of page charges. The article must therefore be hereby marked "*advertisement*" in accordance with 18 U.S.C. Section 1734 solely to indicate this fact.

1987; Sommer and Wurtz 1998; for the SC, see Ottes et al. 1986; Sparks 1978; Sparks et al. 1976).

There is also a more fundamental reason to provide a rigorous quantification of the responses of SNr neurons during saccadic tasks. Evidence from the work of Hikosaka and Wurtz suggests that the saccade-related decreases in the firing rates of SNr neurons are modulated by "contextual" factors, such as whether a target location is visible or remembered or whether a saccade is made inside or outside of a behavioral task (Hikosaka and Wurtz 1983a,c). Although the nature of this context dependence has not been fully explored, it may provide an important clue to the role played by the basal ganglia in movement generation (Evarts et al. 1984). To build on the work of Hikosaka and Wurtz and to further explore the information carried by these neurons under a variety of conditions, a rigorous quantification of nigral response fields is necessary.

Therefore to build on earlier descriptions of SNr response properties, allow a comparison with other oculomotor areas, and facilitate further explorations of the role of the SNr in saccade generation, we attempted to provide a detailed quantitative description of the relationships between the firing rates of SNr neurons and the horizontal and vertical amplitude of upcoming saccades during a visually guided saccade task. For this purpose, we recorded the activity of 72 neurons from the primate SNr while monkeys performed a large number of trials of a delayed saccade task. To sample a wide range of movement amplitudes and directions, on each trial the target was chosen randomly from a wide range of possible locations. To examine changes in neuronal activity throughout the task, on each trial firing rate was measured during five distinct intervals.

Our quantitative analysis led to three novel physiological findings about the SNr. First, we were able to segregate and characterize four distinct classes of saccade-related SNr neurons. Neurons in two of these classes had response properties similar to those described by Hikosaka and Wurtz (1983a–d), but neurons in the other two classes were characterized by saccade-related increases in activity. Second, for the SNr neurons we studied, the relationship between firing rate, in each of the five measured intervals, and horizontal and vertical saccade amplitude could be well described by a planar surface. This planar relationship was qualitatively different from the Gaussian-like relationship between firing rate and horizontal and vertical saccade amplitude than has been found when FEF and SC neurons have been examined in a similar manner (cf. Bruce and Goldberg 1985; Ottes et al. 1986). Finally, our SNr neurons were found to have high trial-to-trial variance in firing rate. In future work, use of planar regressions to quantify the response profile of SNr neurons should prove useful for explorations of the effects of memory, and other behavioral contexts, on the saccade-related activity of SNr neurons.

METHODS

Four male rhesus macaques (*Macaca mulatta*) were used as subjects. All animal procedures were developed in association with the University Veterinarian, approved by the New York University Institutional Care and Use Committee, and designed and conducted in compliance with the Public Health Service's *Guide for the Care and Use of Animals*.

Surgical and training procedures

All surgical and training procedures were performed using standard protocols that have been described in detail elsewhere (Handel and Glimcher 1997). Briefly, in an initial sterile surgery performed under isoflurane inhalant anesthesia, a prosthesis for restraining the head and a scleral search coil (Fuchs and Robinson 1966; Judge et al. 1980) for monitoring eye position were implanted. After this, and all other surgical procedures, animals received analgesics and antibiotics for a minimum of 3 days. After a 6-wk delay, access to water was controlled and subjects were trained to perform oculomotor tasks for juice rewards.

During training and subsequent recording sessions, monkeys were seated, with their heads immobilized, in a primate chair placed 57 in from a tangent screen containing a grid of light emitting diodes (LEDs). These LEDs (441) formed a grid of points, separated by 2° of visual angle, spanning 40° horizontally and 40° vertically.

To gather the data presented in this report, each monkey was trained to produce saccadic eye movements in response to visual stimuli in a delayed saccade task. Each delayed saccade trial (Fig. 1) began with an audible beep. Three hundred milliseconds later a central fixation LED, which appeared yellow to normal human observers, was illuminated and the subject was required to align gaze with this stimulus (±3°) within 1,000 ms. Two hundred to 800 ms after gaze was aligned with this fixation LED, a single yellow eccentric LED was illuminated. After a further 200- to 1,200-ms delay the fixation LED was extinguished (the GO cue), and the subject was required to shift gaze into alignment with the eccentric target LED (±3–5°) within 350 ms. If the subject's gaze remained in alignment with the target for 350–450 ms, the trial was considered to be performed correctly. Each correct trial was reinforced with a 300-ms noise burst which was supplemented randomly with fruit juice on one-third to one-fifth of trials. On each trial, the location of the target was chosen pseudorandomly, with replacement, from the grid of LEDs. All trials were

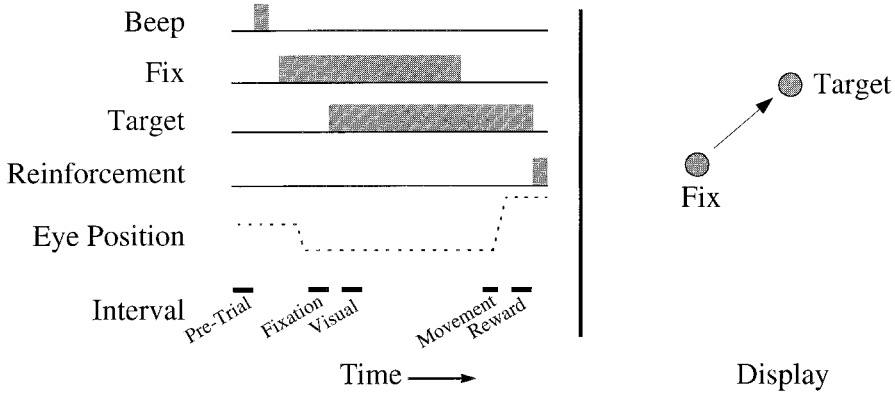

FIG. 1. Temporal sequence of events (*top left*), measured intervals (*bottom left*), and display appearance during a typical delayed saccade task trial in which gaze is shifted from a central fixation point to an eccentric target. Both the target location and the intervals between task events varied randomly. (For details, see METHODS).

performed under dim illumination. Subjects performed the delayed saccade task with an intertrial interval of 200–800 ms.

After a monkey was trained to perform the delayed saccade task, a second sterile surgery was performed to implant a recording chamber allowing vertical electrode penetrations into the SNr. We stereotaxically positioned a stainless-steel receptacle (Crist Instruments) over a 15-mm-diam craniotomy centered 4.5 mm anterior and 7.5 mm lateral to the intersection of the interaural line and the midsaggital plane (on the left side in 3 monkeys and the right side in 1), oriented the receptacle perpendicular to the stereotaxic horizontal plane, and fastened it to the skull with orthopedic bone screws and cement.

Microelectrode recording techniques

After the monkeys were trained to perform the delayed saccade task and had been implanted with a recording chamber, electrophysiological recording sessions were initiated. During each recording session a 23-gauge guide cannula was fixed to an *x-y* micropositioner and used to pierce the dura. A paralyne-coated tungsten microelectrode (Microprobe: 0.5–2.0 MΩ) or a glass-coated platinum-tipped tungsten microelectrode (Ainsworth: 10- to 15-mm exposed tip) was then advanced. Individual action potentials were identified by time and amplitude criteria and the times of occurrence of these action potentials were recorded.

Recording protocol

Following the method of Schultz (Wolfram Schultz, personal communication), we located the SNr in each subject by first recording from neurons of the ventroposterior complex of the somatosensory thalamus. By systematically recording from many locations in the lateral and medial divisions of this complex and determining the location on the animal's body surface that activated each neuron, we were able to construct a topographic map of somatosensory receptive fields of ventroposterior thalamus. Once the region containing neurons with somatosensory receptive fields centered on the lips and mouth was located, we searched for the SNr by vertically advancing electrodes past these neurons and into the underlying tissue. Putative SNr neurons, with 50–125 spikes/s tonic firing rates and oculomotor task-related modulations in activity, typically were first encountered ~2–5 mm ventral to the deepest orofacial somatosensory responses. These neurons were typically encountered while the electrode was advanced for 1–2 mm, after which no further cellular activity was apparent, presumably because the electrode had entered the cerebral peduncle. In some of our more anterior penetrations, when the electrode was extended ventral to neurons with orofacial somatosensory responses, we encountered neurons that were characterized by lower, more variable tonic rates (usually <25 spikes/s) punctuated by saccade-related bursts of activity; the background activity in the neighborhood of these neurons was often more irregular and less vigorous than the background activity in the neighborhood of putative SNr neurons. These low tonic firing rates were inconsistent with Hikosaka and Wurtz's (1983a) descriptions of SNr neurons, as well as our putative SNr neurons, but consistent with Matsumura et al.'s (1992) descriptions of subthalamic neurons. Indeed, marking lesions made at the sites of these neurons were later recovered in the subthalamic nucleus. Thus when we encountered neurons with these physiological properties we tentatively classified them as subthalamic neurons and did not include them in this report.

Data analysis

SINGLE-TRIAL MEASUREMENTS. Data analysis was a three-step process. In the first step, for each correctly executed trial, we measured the horizontal and vertical amplitude of the saccade that aligned gaze with the target as well as the firing rate of the neuron during 5 intervals (Fig. 1): a 200-ms *pre-trial interval* ending at the onset of the beep that initiated the trial; a 200-ms *fixation interval* ending at the onset of the target LED; a 200-ms *visual interval* beginning 50 ms after the onset of the target; a 150-ms *movement interval* beginning 50 ms before the onset of the saccade; and a 200-ms *reward interval* ending at the delivery of reinforcement.

DESCRIPTION OF INDIVIDUAL NEURONS. In the second step of data analysis, for each neuron we examined the relationship between the firing rate during a trial and the horizontal and vertical amplitude of the movement made at the end of the trial. To do this, we generated five *response fields* for each neuron: one response field for each measured interval. Each response field plotted the firing rate of the neuron during the interval as a function of the horizontal and vertical amplitude of the saccade made at the end of each trial.

To quantify the relationship between the firing rate during an interval and the horizontal and vertical amplitude of the saccade made at the end of each trial, we fit each response field with both a planar model (2-dimensional least-squares regression) and a two-dimensional Gaussian model. To compare the efficiencies with which these two models described the data, the proportion of total variance accounted for (VAF) by both the planar and Gaussian fits was computed as (total variance − residual variance)/total variance, where variance was defined as the sum of the squared Cartesian distances between the data and *zero*.

An F test was performed to determine if each planar fit was significantly tilted. We also examined the planar fits to determine if they consistently under- or overestimated firing rate for any particular range of movement amplitudes and directions. To do this, we calculated the firing rate predicted by the regression and subtracted it from the observed firing rate of the neuron. We then averaged these *residuals* into $4 \times 4°$ bins and plotted them as a function of horizontal and vertical movement amplitude.

The Gaussian models had six free parameters: baseline rate, peak modulation, horizontal and vertical centers, and horizontal and vertical standard deviations. For each response field fit with the Gaussian model, baseline rate was constrained to lie between 0 spikes/s and the maximum firing rate observed on any trial during that interval. The horizontal and vertical centers of the function were constrained to be within the range of movements we sampled (i.e., between −20 and +20°) while the horizontal and vertical standard deviations were constrained to lie between 4 and 40°. Parameters of the model were estimated using a Nelder-Meade simplex iterative fit that minimized the squared Cartesian distance between the Gaussian model and the raw data (Matlab). The optimization procedure was run for 10,000 iterations on each of 10 sets of initial seed parameters. Because the Gaussian fits never significantly outperformed the linear regressions, as will be described in RESULTS, we used the parameters of the planar fits in subsequent stages of analysis.

For some neurons, perievent time histograms also were generated to examine the temporal relationships between modulations in neuronal activity and significant task events. For each perievent time histogram, we took the average firing rate, in 25-ms bins, across many trials ending with movements of similar amplitudes and directions and plotted those average rates as a function of time (±SD and ±SE). Four 400-ms histograms were generated for each neuron, centered, respectively, on the time when the monkey aligned gaze with the central LED, the time when the target LED was illuminated, the time when the saccade required for reinforcement began, and the time when reinforcement was delivered.

CLASSIFICATION OF NEURONS. By informally examining single trials and response fields for each neuron, we found that nigral neurons exhibited one of four basic response profiles during the delayed saccade task: a decrease in firing rate after target onset and/or before saccade onset on trials ending with contraversive movements, a decrease in firing rate that began after fixation and continued until the delivery of reinforcement on *all* trials, an *increase* in firing rate after target onset and/or before saccade onset on trials ending with

contraversive movements, and an increase in firing rate after target onset and/or before saccade onset on trials ending with contraversive saccades and a decrease in firing rate on trials ending with ipsiversive saccades.

These four response profiles could be distinguished by whether firing rate increased or decreased during each interval, and we used this property to systematize our classification scheme. First, we computed a measure of the tonic baseline firing rate of each neuron by calculating the mean and standard deviation of the firing rate during the pre-trial interval across all trials. Then for each of the other four measured intervals, we calculated the percentage of trials in which the firing rate during the interval was ≥1.5 SD below baseline. Because baseline firing rate was normally distributed for most neurons, this threshold would be exceeded on only slightly >6% of trials for neurons with random rate modulations. To identify neurons that paused in a nonrandom manner, we therefore defined a neuron as *pausing* during an interval if decreases in activity of ≥1.5 SD occurred on >12% of trials (see Handel and Glimcher 1997). Similarly, we defined a neuron as *bursting* during an interval if there were significant increases in activity (≥1.5 SD above baseline) on >12% of trials. Neurons then were assigned to classes based on the intervals in which they paused and burst. Neurons that paused during the visual or movement interval, but did not pause during all intervals, were classified as *discrete pausers*. Neurons that paused during *all* intervals were classified as *universal pausers*. Neurons that burst during the visual or movement intervals were classified as *bursters*. Finally, the small number of neurons that both paused and burst during the visual and/or movement intervals were classified as *pause-bursters*.

When we used alternate methods (for details, see DISCUSSION) to sort SNr neurons into categories, we consistently found four separable groups, and nearly all of the same neurons were grouped together by each of the classification methods we employed. Perhaps most importantly for this characterization of the reticulata population, the modal characteristics of the group of neurons assigned to each class were robust; they essentially were unaffected by changes in the classification criteria.

POPULATION ANALYSES. The third step of data analysis was a population level description of SNr neurons. We described the characteristics of the neurons assigned to each cell class by extracting the relative *z* intercepts, the slope magnitudes, and slope directions from the regression planes fit to the response fields generated for each neuron. These parameters provided estimates of the intervals during which the average firing rates of the neurons were modulated up or down, the degree to which these modulations were linearly related to horizontal and vertical saccade amplitude, and the movement directions associated with the largest modulations. Histograms and polar plots of these values were then prepared and these data were tested for statistical significance.

Histology

The locations of recording sites were identified histologically in two monkeys. During the 2 wk before the animals were killed, electrolytic marking lesions were made at the sites where the activity of single neurons was recorded. Lesions were made by passing a 5 μA anodal current through the tip of the recording electrode for 5–10 s. At the end of this 2-wk period, the animals were premedicated with ketamine and then killed with an overdose of thiopental sodium. They were perfused intracardially with a saline solution followed by 4% paraformaldehyde in phosphate buffered saline and finally by 30% sucrose in phosphate buffered saline. The brains were removed from the skulls, submerged in 30% sucrose for 3 days, blocked and cut into 40-μm frozen sections. The sections then were mounted and stained with thionine, and the anatomic locations of the lesions were identified, photographed, and recorded on camera lucida reconstructions of the sections.

RESULTS

We examined 72 saccade-related neurons in this study. Each neuron was examined while subjects correctly executed 50–500 delayed saccade trials (136 ± 80; mean ± SD). After all the neuronal data were collected, each neuron was classified as described in METHODS. For each cell class, we present data for a single neuron having near modal response properties. We then present a population level analysis of all the neurons in the class.

Discrete pausers

SINGLE NEURON DATA. Thirty-five percent of the SNr neurons we studied ($n = 25$) were classified as discrete pausers. Figure 2 plots the activity of a typical discrete pauser during two delayed saccade trials. Horizontal and vertical eye position is plotted as a function of time above the instantaneous firing rate of the neuron. At the end of one trial (*left*), the monkey made a downward and contraversive saccade. Note that shortly after the onset of this target, firing rate decreased to nearly zero and continued at this lower level until the saccade. During another trial (*right*), at the end of which the monkey made an upward and ipsiversive saccade,

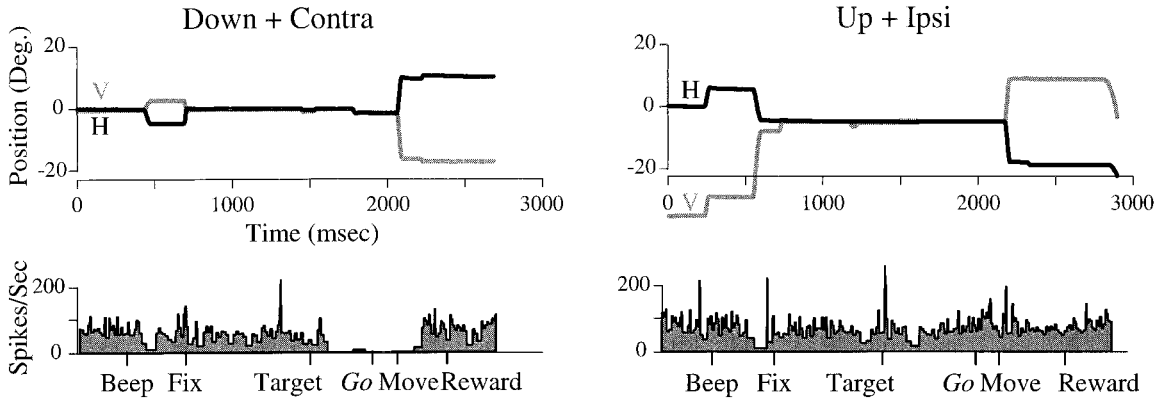

FIG. 2. Eye position (*top*) and instantaneous firing frequency of a typical discrete pauser (*bottom*) are plotted as a function of time during 2 delayed saccade trials, 1 ending with a contraversive and downward saccade (*left*) and the other ending with an ipsiversive and upward saccade (*right*). Tick marks indicate the onset times of the trial (Beep), fixation (Fix), the target (Target), the initiation cue (GO), the movement (Move), and reinforcement (Reward).

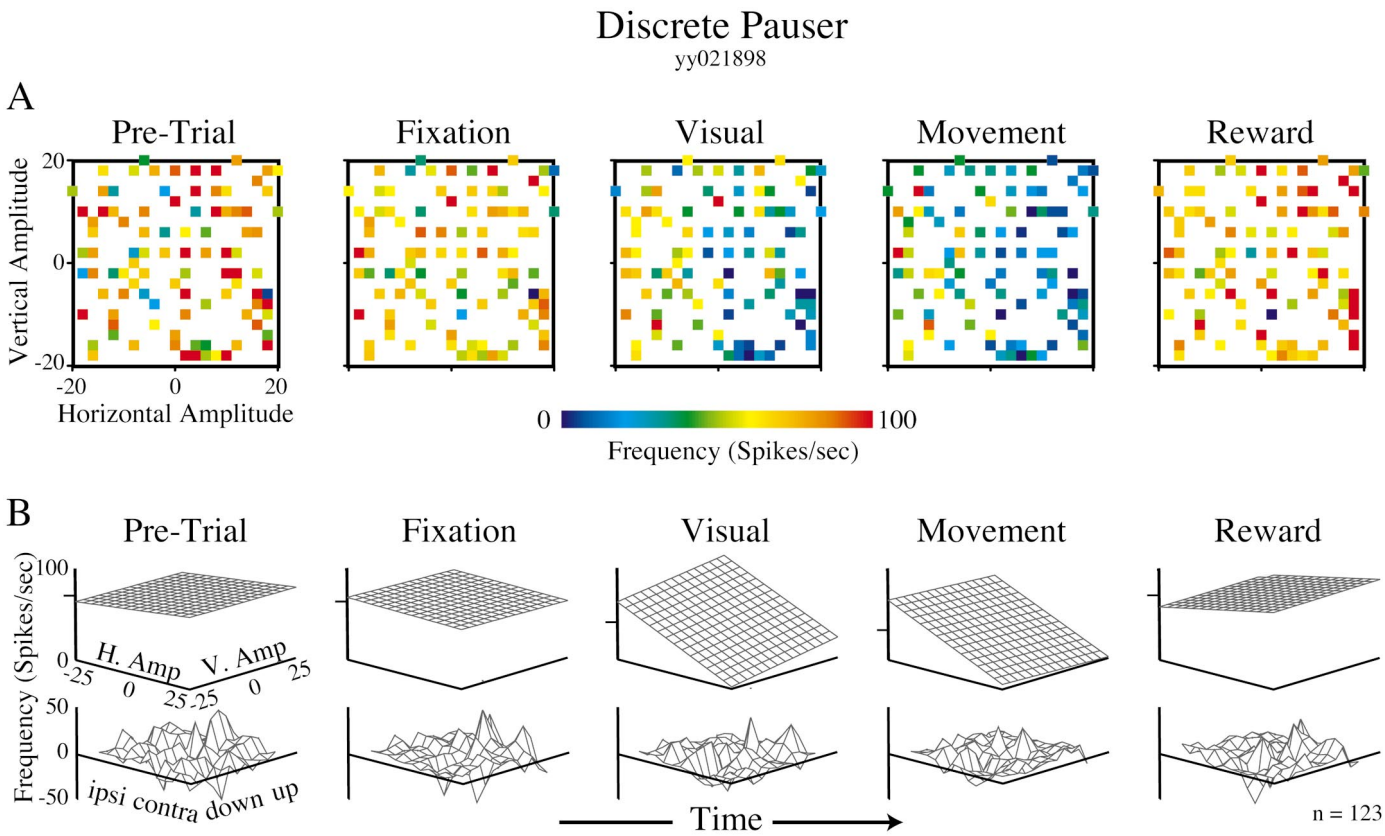

FIG. 3. *A*: response fields plotting the firing rate of a typical discrete pauser during the pre-trial, fixation, visual, movement, and reward intervals as function of the horizontal and vertical amplitude of the reinforced saccade. Data were averaged into 2 × 2° bins. *B*: planar fits to the response fields in *A* (*top*) and plots of the differences between the observed and predicted spike rates on each trial (*bottom*). Planar intercepts (shown graphically as tick marks on *z* axes) from left to right: 72, 66, 43, 34, and 73 spikes/s. Slope magnitudes: 0.3 , 0.1, 1.3, 1.2, and 0.5 spikes · s^{-1} · deg^{-1}. Slope directions (uphill): 184, 10, 342, 4, and 189°.

the firing rate of the neuron remained near baseline throughout the trial.

We recorded the activity of this neuron during 123 delayed saccade trials. From these data we generated response fields that plot the firing rate of the neuron, coded in color, as a function of the horizontal and vertical amplitude of the saccade made at the end of the trial for the pre-trial, fixation, visual, movement, and reward intervals (Fig. 3*A*). Note that during the visual and movement intervals, the firing rate of the neuron was depressed below the mean baseline level for most trials but was consistently lower on trials terminating with downward and contraversive saccades than on trials terminating with upward and ipsiversive saccades.

In Fig. 3*B* the optimally fit plane for each response field is presented above the residuals for those fits. Note that there is no systematic spatial structure to any of the residuals, indicating that these computed planes do not systematically misrepresent the firing rate of the neuron. Further, in all intervals these planar fits account for the firing rate of the neuron as well as our 6 parameter Gaussian model did (see Table 1). In fact, planar fits performed as well as Gaussian fits at accounting for the firing rates of almost all the nigral neurons we analyzed, during all measured intervals (see Table 1). Therefore we used parameters from these planar fits to determine the intervals during which the firing rate of the neuron was modulated, whether any modulations in neuronal activity were correlated

TABLE 1. *Percent variance accounted for by planar/Gaussian fits*

	Fixation	Visual	Movement	Reward
Single example neurons				
Discrete pauser	92/92	81/80	79/80	94/94
Universal pauser	92/92	87/87	54/54	89/90
Burster	91/91	91/91	94/94	97/97
Pause-burster	92/92	89/89	95/95	97/97
Population by class				
Discrete pausers	91 ± 8/92 ± 7	89 ± 10/89 ± 10	88 ± 8/88 ± 8	94 ± 3/95 ± 1
Universal pausers	84 ± 11/84 ± 11	80 ± 12/81 ± 11	71 ± 21/73 ± 20	79 ± 20/81 ± 20
Bursters	90 ± 9/90 ± 9	92 ± 6/93 ± 5	92 ± 7/92 ± 7	94 ± 4/95 ± 3
Pause-bursters	91 ± 6/91 ± 6	91 ± 7/93 ± 4	92 ± 8/93 ± 4	95 ± 5/96 ± 5

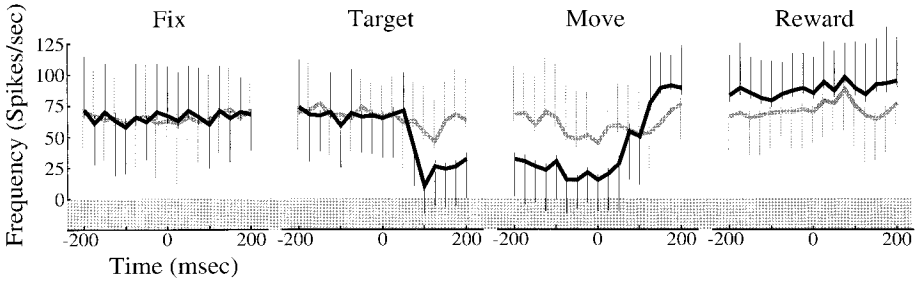

FIG. 4. Perievent time histograms for a typical discrete pauser during 40 trials ending with contraversive (black: horizontal target position ranged from 10 to 20° rightward) and 37 trials ending with ipsiversive (gray: horizontal target position ranged from 10 to 20° leftward) saccades. Histograms plot the mean (vertices), SD (long bars), and SE (short bars) of firing rate in 25-ms bins aligned on fixation, target onset, movement onset, and reinforcement (for details, see text).

with the horizontal and vertical amplitude of the movement at the end of the trial, and the magnitude and orientation of any of these spatially dependent neuronal modulations.

To determine whether the average activity of this discrete pauser differed from baseline during an interval, we compared the average firing rate of the neuron (the *z* intercept from the planar fit) during the interval with the average firing rate of the neuron during the pre-trial interval. On average, this discrete pauser fired at 70 spikes/s before trials began. During the visual and movement intervals, the average firing rate of the neuron decreased substantially but returned to the baseline level during the reward interval.

To examine whether there was a systematic relationship between the firing rate of the neuron and the horizontal and vertical amplitude of the saccade made at the end of the trial, we determined whether there was a significant tilt to the regression planes fit to the response fields for each interval. In the pre-trial and fixation intervals, the planes were not significantly tilted. However, in the visual and movement intervals, the planar fits were significantly tilted ($P < 0.001$). Finally, in the reward interval, when the average firing rate of the neuron had returned to baseline, the planar fit was no longer significantly tilted ($P = 0.07$).

We also examined the steepness and orientations of the tilts of the best-fit planes. For both the visual and movement intervals, the regression planes were oriented so that they sloped downhill into the contraversive hemifield (maximum positive gradients, or *uphill* slope directions, for the visual and movement intervals: 342 and 4°, respectively, where 0° is defined as ipsiversive) and were relatively steep. This indicates that the firing rate of the neuron was ~50 spikes/s lower on trials terminating with the largest amplitude contraversive saccades we sampled than on trials terminating with the largest amplitude ipsiversive saccades we sampled.

Figure 4 plots four perievent time histograms aligned on the times at which the subject fixated the central LED, the target LED was illuminated, the saccade aligning gaze with the target began, and reinforcement was delivered. Note that on trials in which the subject made contraversive movements (plotted in black), the neuron paused after target onset and continued at this lower rate of firing until shortly after movement onset. In contrast, the average firing rate of the neuron was largely unchanged during trials in which the subject made ipsiversive movements (plotted in gray). It is also noteworthy that, although the average firing rate was ~70 spikes/s around the time of fixation for both sets of trials, there was substantial

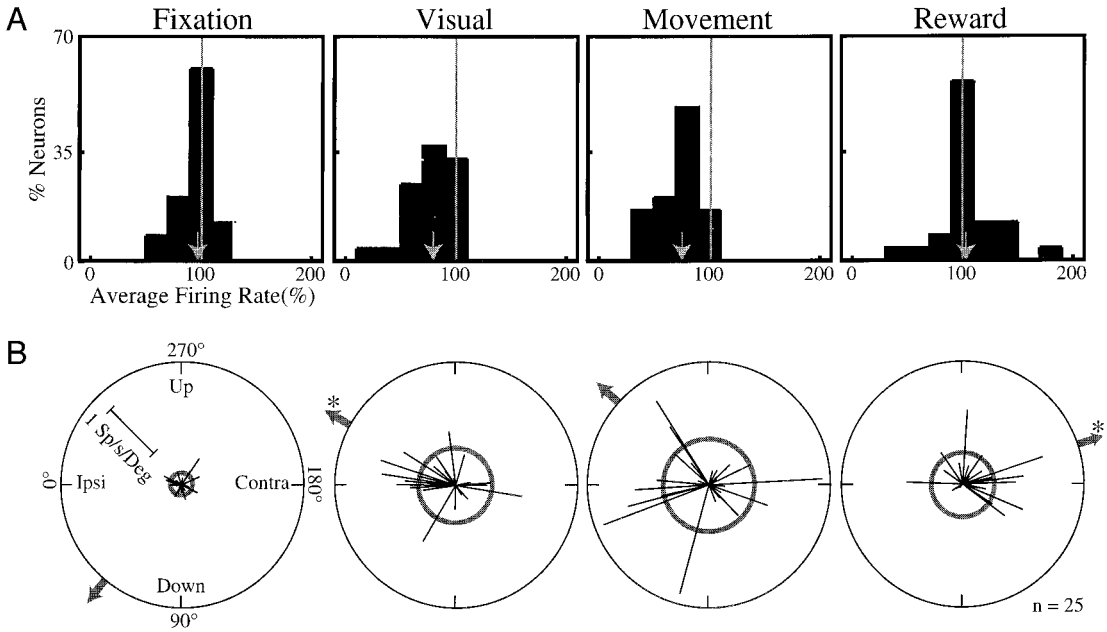

FIG. 5. Parameters from the planar fits to the response fields of 25 discrete pausers measured during the fixation, visual, movement, and reward intervals. *A*: histograms of average firing rate, estimated by the *z* intercepts of the planar fits, plotted as a percentage of baseline for each of the 4 intervals. Means ± SD (gray arrows): 96 ± 15, 78 ± 19, 74 ± 17, and 105 ± 26%. *B*: polar plots of planar slopes. Mean slope magnitudes during the 4 intervals (gray circles) were: 0.18 ± 0.11, 0.61 ± 0.35, 0.76 ± 0.58, and 0.53 ± 0.38 (SD) spikes · s^{-1} · deg^{-1}. Mean slope directions (gray arrows) were: 50, 330, 318, and 199°. Slope directions which formed a significant uniform distribution ($P < 0.05$) by the Rayleigh test are marked with an asterisk.

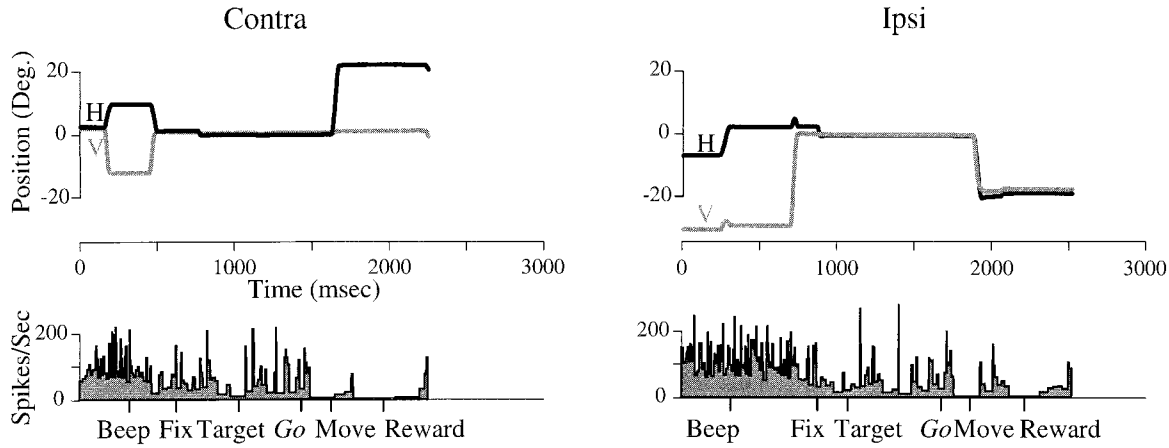

FIG. 6. Activity of a typical universal pauser during 2 delayed saccade trials. Plots are constructed similarly to those in Fig. 2.

trial-to-trial variance (long error bars indicate 1 SD). This high trial-to-trial variability was not limited to periods when the cell was firing at a tonic rate but also could be seen during periods of rate modulations.

POPULATION ANALYSES. As shown in Table 1, planar linear regressions were good descriptors of the relationship between neuronal firing rate and horizontal and vertical saccade amplitude for all 25 neurons we classified as discrete pausers. For each neuron we compared the average firing rate (the *z* intercept from each planar fit) during the fixation, visual, movement, and reward intervals with the average firing rate during the pre-trial interval to determine the degree to which the firing rates of each discrete pauser were modulated in each interval (a property that could not be predicted from our classification criteria). Figure 5*A* plots histograms of average firing rate as a percentage of baseline for all 25 discrete pausers. During the fixation interval, the firing rate of the neurons remained close to baseline. Not surprisingly, average firing rate did drop below baseline during the visual and movement intervals, though it is noteworthy that the decreases were of similar magnitude in both intervals. Finally, in the reward interval, the firing rates of discrete pausers tended to return to, or slightly exceed, baseline levels.

To determine whether these changes in average neuronal activity varied with horizontal and vertical saccade amplitude and/or with horizontal and vertical target position, we first determined whether the regression planes in each interval were significantly tilted. During the fixation interval when no relationship between firing rate and the horizontal and vertical amplitude of the, as yet, unspecified movement could be expected, the tilt was significant ($P < 0.05$) for only 1 of the 25 neurons (4%). However, planar regressions were significantly tilted for 20 neurons (80%) during the visual interval, 19 neurons (76%) during the movement interval, and 14 neurons (56%) during the reward interval.

Next, to examine the orientations and magnitudes of these spatially tuned responses, we generated polar plots (Fig. 5*B*) of the uphill directions and magnitudes of the slopes of the regression planes from each interval for all 25 discrete pausers. In the fixation interval, the tilts of the regression planes were, unsurprisingly, shallow and were not consistently oriented in any direction ($P > 0.8$ using the Rayleigh test for the unimodal distribution of a circular variable) (cf. Batschelet 1981). In the visual interval, however, the regression planes had steeper tilts, so that, on average, there was an approximately 25-spikes/s difference in response rate for movements at the highest and lowest points on each planar fit within our sampling range. Moreover, the tilts of these planes were consistently oriented in the same direction from neuron to neuron ($P \cong 0.05$). The average planar fit was oriented so that the *uphill* direction was ipsiversive and slightly upward (330°), indicating that, on average, these discrete pausers were *least* active before large-amplitude contraversive, and slightly downward, movements. During the movement interval, neuronal responses also were modulated as a function of horizontal and vertical saccade amplitude. The tilts of the planar fits for this interval were even steeper but the orientations of these planes were more variable. The mean uphill direction (318°) was similar to that seen in the visual interval, but the slope directions did not form a significant unimodal distribution (Rayleigh $P \cong 0.78$). Finally, during the reward interval, the average tilt of the planes was shallower, and the slope directions formed a unimodal distribution (Rayleigh $P \cong 0.05$) around an average uphill direction of 199°, that is, into the opposite horizontal hemifield from the direction observed during the visual and movement intervals. Thus during the reward interval, discrete pausers tended to have ~20 spikes/s higher firing rates after 20° contralateral movements than after 20° ipsilateral movements. Note that the estimates of mean firing rate as percentages of baseline during this interval were often >100% because, after pausing, the firing rates of many discrete pausers transiently increased. For these neurons, the same large-amplitude contralateral movements that produced the deepest visual and movement interval pauses also were followed by the largest reward interval increases in activity.

These population analyses indicate that the firing rates of the group of neurons we classified as discrete pausers tended to decrease during the interval between target onset and movement onset and that these decreases were more substantial during trials ending with contraversive movements than during trials ending with ipsiversive movements.

Universal pausers

SINGLE NEURON DATA. Twenty-four percent of the SNr neurons we studied ($n = 17$) were classified as universal pausers. Figure 6 plots the activity of a typical universal pauser during

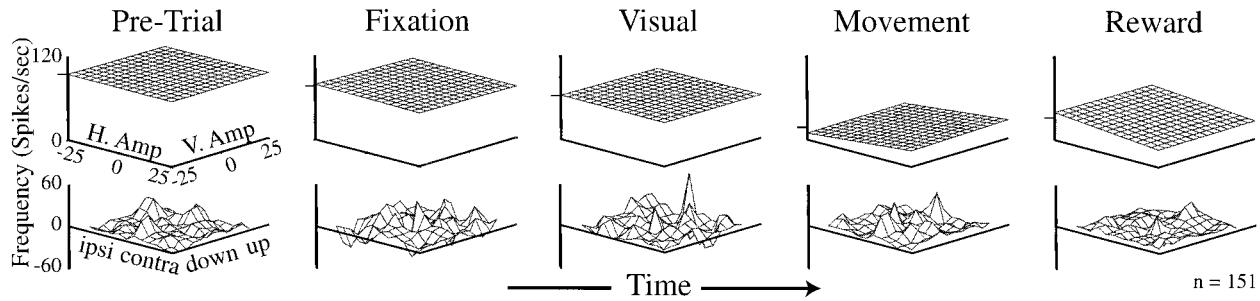

FIG. 7. Surfaces derived from planar fits, as well as associated residuals, for the response fields of a typical universal pauser. Plots were constructed similarly to those in Fig. 3*B*. Planar intercepts (estimates of mean firing rate): 95, 77, 64, 18, and 33 spikes/s. Slope magnitudes: 0.1, 0.1, 0.0, 0.3, and 0.3 spikes $\cdot s^{-1} \cdot deg^{-1}$. Slope directions (uphill): 317, 5, 331, 198, and 353°.

two delayed saccade trials; one ending with a contraversive saccade and the other with an ipsiversive saccade. During both trials, the neuron fired action potentials at a high rate until the monkey aligned gaze with the central LED. After this fixation, the firing rate of the neuron decreased and remained below baseline until the trials ended. Note that the instantaneous firing frequency of the neuron did not decrease smoothly after fixation but became highly variable, although in both trials the neuron was practically inactive just before the movement and around the time reinforcement was delivered.

Figure 7 plots the best-fit planes and residuals for the five measured intervals. Note that there was very little spatial structure apparent in the residuals in any interval, indicating that these planes did not systematically misrepresent the firing rate of the neuron. Furthermore in all intervals, these planar fits accounted for the firing rate of the neuron as well as our Gaussian model (Table 1).

For each interval, we determined whether the activity of the neuron was modulated from baseline by examining the average firing rate across all trials as determined by the linear fits. After the monkey fixated the central LED, the average firing rate dropped by ~20 spikes/s and continued to decrease until around the time of the saccade, remaining substantially below baseline during the reward interval. We also used the planar fits to determine whether there was a systematic relationship between these modulations and the horizontal and vertical amplitudes of the movements produced at the end of the trials. We found that the tilt of the regression plane nearly reached significance in the movement interval ($P \cong 0.05$) and did reach significance during the reward interval ($P < 0.001$). To determine how strongly the firing rate of this universal pauser was modulated by the horizontal and vertical amplitude of the movement during these intervals, we examined the steepness of the regression slopes. We found that the tilts of the regression slopes were relatively shallow during both these intervals. Thus the modulation in activity that we observed was essentially independent of the horizontal and vertical amplitude of the movement produced at the end of the trial.

Because, during all intervals, the activity of this universal pauser was not substantially modulated by the horizontal and vertical amplitude of the movement, we averaged the firing rates from all 151 delayed saccade trials to produce the four perievent time histograms shown in Fig. 8. Note the gradual decline in firing rate that begins after fixation onset and becomes more pronounced before movement onset. Both during periods when the average firing rate of the neuron was near baseline and during periods when the average firing rate was significantly below baseline, the trial-to-trial variance in firing rate for this universal pauser was substantial.

POPULATION ANALYSES. Although our definition of universal pausers ensures that the average firing rates of these neurons decrease below baseline during all intervals, the magnitude of these decreases cannot be predicted by our classification criteria. The average depths of the decreases we did observe can be seen in the histograms in Fig. 9*A* that plot mean firing rates as a percentage of baseline for all 17 universal pausers. Although the firing rates of all universal pausers decreased from baseline during all postbaseline intervals, these decreases tended to be smallest during the fixation interval. In the visual, movement, and reward intervals, the decreases in activity tended to be more substantial; in all three of these intervals, the mean firing rate of universal pausers dropped to half of the baseline value.

To determine whether the depths of these decreases in firing rate were modulated by the horizontal and vertical amplitude of the movement made at the end of the trial, first we determined whether the regression planes in each interval were significantly tilted. During the fixation interval 18% of the planes were significantly tilted. In the visual, movement, and reward intervals, when the activity of the neurons was deeply suppressed and saccadic targets were visible, 47, 53, and 65% of the planes were tilted significantly.

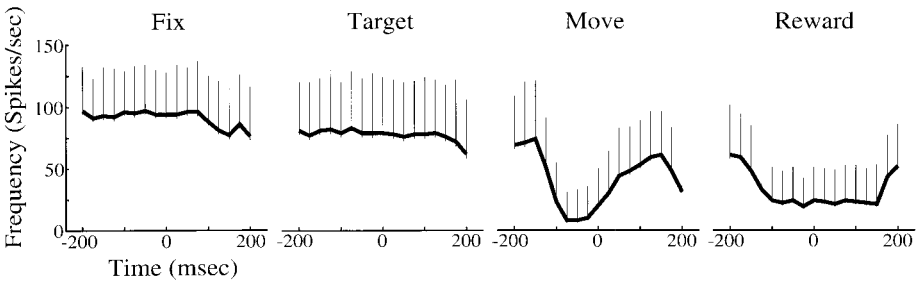

FIG. 8. Perievent time histograms for a typical universal pauser plotting the average firing rate with SD and SE during all 151 trials, regardless of saccadic amplitude and direction. Plots were constructed similarly to those in Fig. 4.

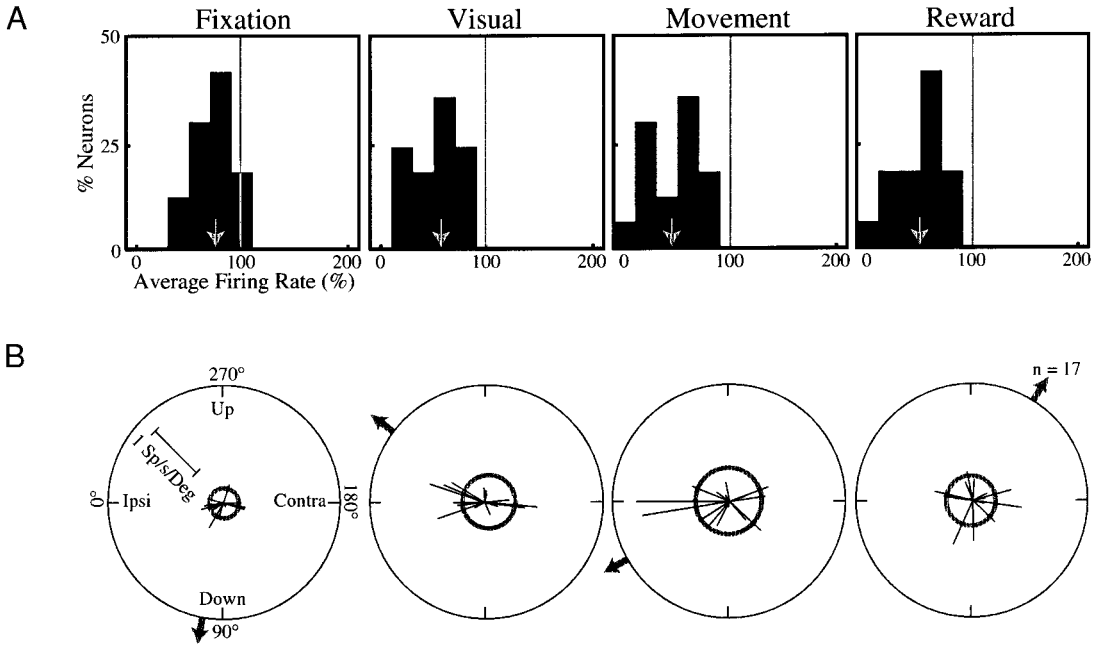

FIG. 9. Parameters from the planar fits to the response fields of 17 universal pausers during the fixation, visual, movement, and reward intervals. Plots were constructed similarly to those in Fig. 5. *A*: histograms of planar intercepts plotted as percentage of baseline. Means ± SD (gray arrows): 73 ± 17, 55 ± 22, 45 ± 25, and 51 ± 24%. *B*: polar plots of planar slopes. Mean magnitudes (gray circles): 0.26 ± 0.14, 0.46 ± 0.30, 0.58 ± 0.42, and 0.43 ± 0.25 spikes · s^{-1} · deg^{-1}. Mean directions (gray arrows): 80, 324, 30, and 238°.

Figure 9*B* plots the direction and magnitude of the slopes of the regression planes from each interval for all 17 universal pausers. In the fixation interval, the regression planes tended to have relatively shallow tilts and were not consistently oriented in the same direction from neuron to neuron (Rayleigh $P \cong 0.25$). In the visual, movement, and reward intervals, the planes tended to be steeper but the orientations of the regression slopes did not form significant unimodal distributions in either the visual, movement, or reward intervals (Rayleigh $P \cong 0.25$, 0.60, and 0.72). It is important to note, however, that the firing rates of universal pausers decreased on all trials regardless of the amplitude and direction of the saccade.

Thus although the firing rates of all universal pausers decreased substantially during all postbaseline intervals, the size of these decreases depended significantly on the horizontal and vertical amplitude of the saccade made at the end of the trial in only about half the neurons. Moreover this spatial dependence was relatively weak in comparison with the overall decreases in rate from baseline. Finally, the weak spatial dependence that was observed in some universal pausers did not have a consistent orientation from neuron to neuron.

These population analyses indicate that the firing rate of the group of neurons we classified as universal pausers tended to be suppressed significantly below baseline during all measured intervals, that for all universal pausers, these pauses in activity were present on all trials, regardless of the amplitude and direction of the saccade made at the end of the trial, and that for some universal pausers, the size of these pauses was modulated by the amplitude and direction of the saccade made at the end of the trial, but the strength of these modulations was relatively weak, and the orientations of their spatial dependence were inconsistent.

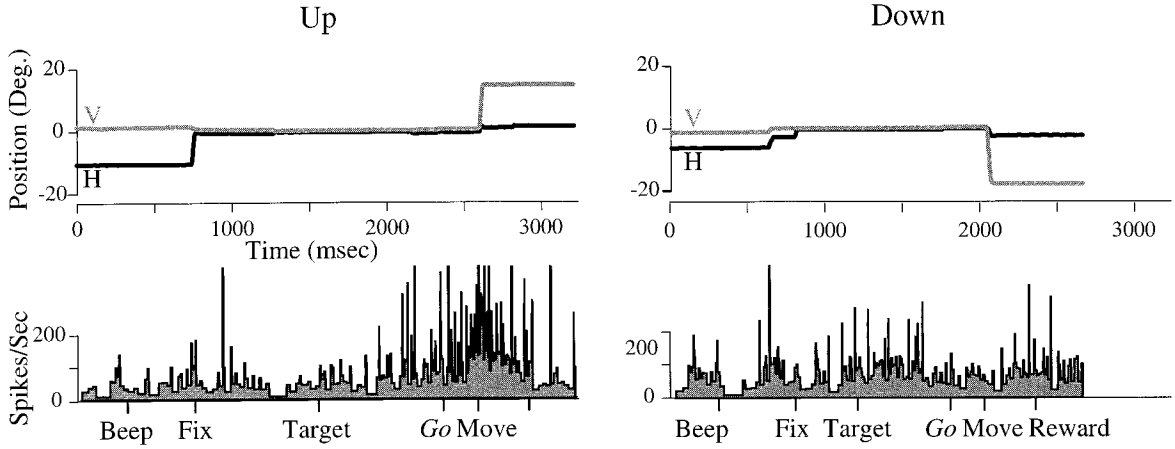

FIG. 10. Activity of a typical burster during 2 delayed saccade trials, 1 ending with an upward saccade (*left*) and the other ending with a downward saccade (*right*). Plots are constructed similarly to those in Fig. 2.

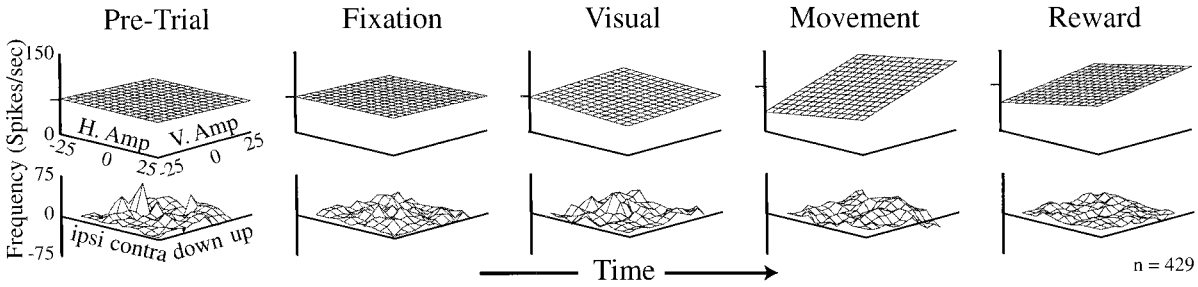

FIG. 11. Surfaces derived from planar fits, as well as associated residuals, for the response fields of a typical burster. Plots were constructed similarly to those in Fig. 3*B*. Planar intercepts (estimates of mean firing rate): 63, 66, 66, 83, and 86 spikes/s. Slope magnitudes: 0.1, 0.1, 0.3, 1.4, and 0.9 spikes $\cdot s^{-1} \cdot deg^{-1}$. Slope directions (uphill): 78, 121, 313, 247, and 219°.

Bursters

SINGLE NEURON DATA. Thirty percent of the neurons we studied ($n = 22$) were classified as bursters. Figure 10 shows the activity of a typical burster during two delayed saccade trials. At the end of one trial (*left*), the monkey made an upward saccade. Before the saccade, neuronal firing rate increased and remained at an elevated level until reinforcement was delivered. During another trial (*right*), at the end of which the monkey made a downward saccade, the firing rate of the neuron remained constant.

When we examined the response fields of the neuron during each interval (Fig. 11), we found that during the movement and reward intervals the average firing rate of the neuron increased substantially. To determine whether there was a systematic relationship between the firing rate of the this neuron and the horizontal and vertical amplitudes of the movements produced at the end of the trials, we examined the significance of any tilt in the planar fits. During the visual, movement, and reward intervals, the firing rate of the neuron was correlated significantly with horizontal and vertical saccade amplitude (visual interval: $P = 0.02$, movement and reward intervals: $P < 0.001$). To evaluate the magnitudes and orientations of the relationship between firing rate in these intervals and the horizontal and vertical amplitudes of the movement made at the end of the trial, we examined the steepness and orientations of the tilts of the regression planes for each interval. In the visual interval the tilt of the plane, though significant, was relatively shallow. However, in the movement and reward intervals, the regression planes were steeply tilted and were oriented so that the uphill direction was upward and contraversive. Thus the planar fits indicate that the firing rate of this neuron was ~60 spikes/s higher during the movement interval and 40 spikes/s higher during the reward interval on trials ending with large-amplitude upward contraversive movements than on trials ending with large-amplitude downward ipsiversive movements.

Figure 12 plots perievent histograms that average the firing rates of the neuron during 144 trials ending with upward saccades (in black) and 121 trials ending with downward saccades (in gray). Note the increase in firing rate at movement onset for trials with upward saccades that is followed by a decrease in activity after the reward on all trials. As with other SNr neurons, there was substantial trial-to-trial variance in the firing rate of this burster that was present in nearly all bins, regardless of the average firing rate.

POPULATION ANALYSES. Figure 13*A* plots histograms of average firing rates, as a percentage of baseline, for all 22 bursters. There was a slight tendency for the firing rate of bursters to increase after fixation. During the visual and movement intervals, the average firing rates of bursters tended to increase by about one-third. These increases in activity usually grew larger by the time reinforcement was delivered, although our population of bursters varied widely in this respect. During the fixation interval, the tilt of the best fit plane was significant for only 9% of the bursters. However, during each of the visual, movement, and reward intervals, the planes for 64% of our bursters were significantly tilted. Figure 13*B* plots the directions and magnitudes of the slopes of the regression planes from each interval. During the fixation interval, the regression planes had relatively shallow tilts and were not consistently oriented in any direction (Rayleigh $P \cong 0.42$). However, during the visual, movement, and reward intervals, the tilts of the regression planes were steeper. Moreover, during these intervals the planes tended to be oriented so that the uphill slopes pointed into the contraversive hemifield, although the slope directions comprised a significant unimodal distribution only in the visual interval (Rayleigh $P \cong 0.01, 0.12, 0.81$). Thus the planar fits indicated that, during the visual, movement, and reward intervals, on average bursters tended to fire action potentials at a rate 25–35 spikes/s higher on trials ending with large-amplitude contraversive saccades than on trials ending with large-amplitude ipsiversive saccades. Note that although the regression planes tended to be oriented in the opposite direction for bursters and discrete pausers, this is only because the regression slopes point *uphill*, toward the movements associated with the smallest decreases in the firing rates of discrete pausers and the movements

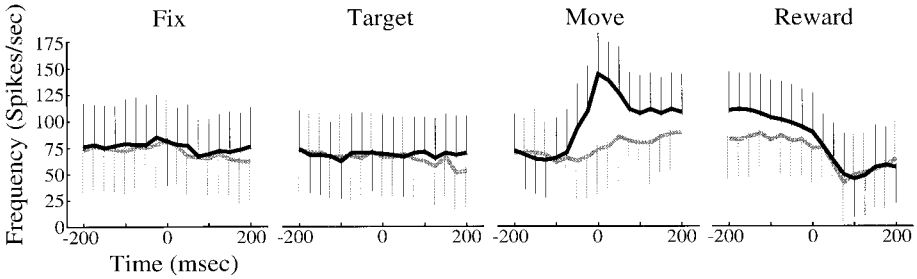

FIG. 12. Perievent time histograms for a typical burster plotting the average firing rate with SD and SE during 144 trials ending with upward (black: vertical target position ranged from 10 to 20° upward) and 121 trials ending with downward (gray: vertical target position ranged from 10 to 20° downward) saccades. Plots were constructed similarly to those in Fig. 4.

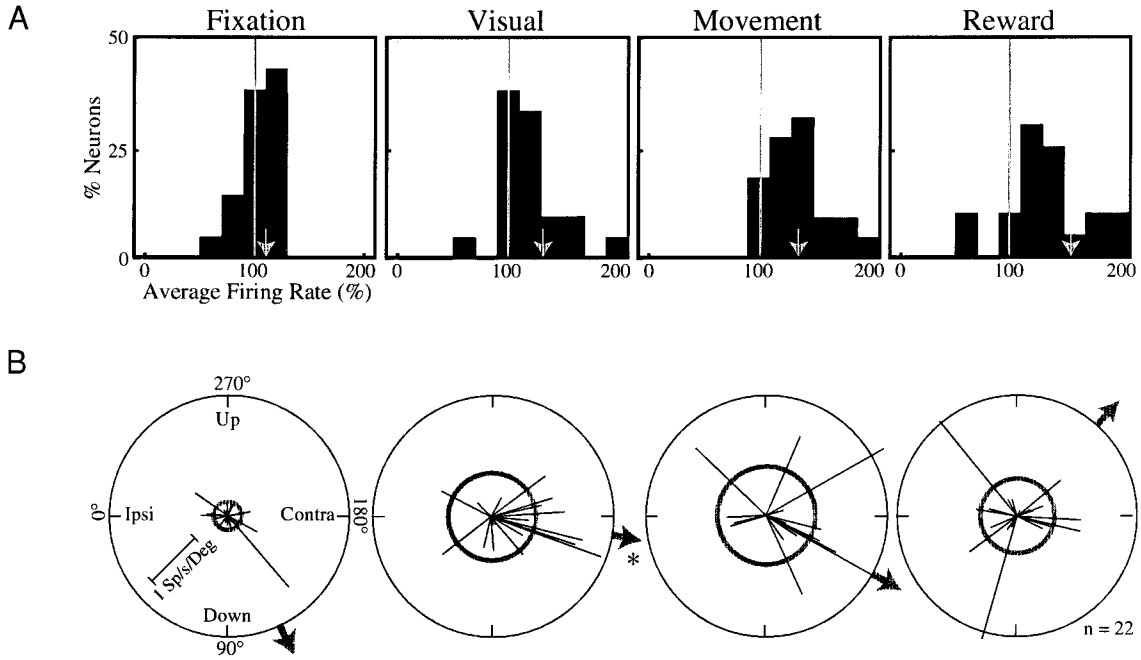

FIG. 13. Parameters from the planar fits to the response fields of 22 bursters during the fixation, visual, movement, and reward intervals. Plots were constructed similarly to those in Fig. 5. *A*: histograms of planar intercepts (plotted as a percentage of baseline). Means ± SD (gray arrows): 111 ± 36, 130 ± 57, 136 ± 28, and 154 ± 82%. *B*: polar plots of planar slopes. Mean magnitudes (gray circles): 0.29 ± 0.32, 0.73 ± 0.52, 0.82 ± 0.62, and 0.63 ± 0. 55 spikes · s^{-1} · deg^{-1}. Mean directions (gray arrows): 115, 171, 151, and 228°.

with the largest increases in the firing rates of bursters. Both classes of neurons tended to generate the largest modulations on trials terminating with large-amplitude movements into the contraversive hemifield.

These population analyses indicate that the group of neurons we classified as bursters tended to generate increases in firing rate after the onset of the target LED and before the beginning of the saccade; these increases in activity were sustained until the delivery of reinforcement; and these increases in activity tended to be larger on trials ending with contraversive saccades than on trials ending with ipsiversive saccades.

Pause-bursters

SINGLE NEURON DATA. Eleven percent of the SNr neurons we studied ($n = 8$) were classified as pause-bursters (see METHODS). Figure 14 plots the activity of a typical pause-burster during two delayed saccade trials. At the end of one trial (*left*), the monkey made a small amplitude downward saccade. Shortly after target onset the firing rate of the neuron increased abruptly, reached a peak of activity just before the movement, and continued to fire at an elevated rate until the end of the trial. During another trial (*right*), at the end of which the monkey made an ipsiversive saccade, the neuron ceased firing action potentials shortly after the target was illuminated and did not resume firing at the baseline rate until just before the onset of the saccade.

Note that the regression planes do not completely capture the systematic spatial structure of the firing rate of this neuron (Fig. 15). The residual plots for the visual and movement intervals reveal that the regression planes consistently underestimate the firing rate of the neuron on trials terminating with small-amplitude downward movements.

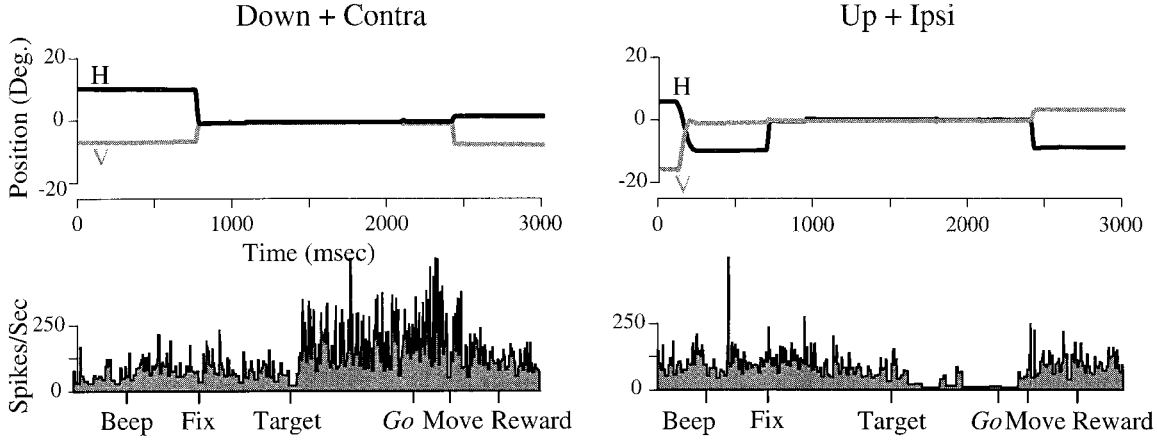

FIG. 14. Activity of a typical pause-burster during 2 delayed saccade trials, 1 ending with a contraversive and downward saccade (*left*) and the other ending with an ipsiversive and upward saccade (*right*). Plots are constructed similarly to those in Fig. 2.

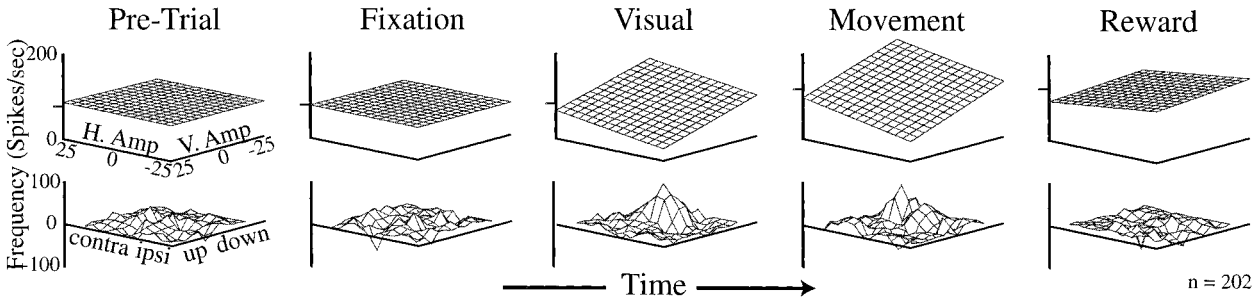

FIG. 15. Surfaces derived from planar fits, as well as associated residuals, for the response fields of a typical pause-burster. Plots were constructed similarly to those in Fig. 3*B*. Planar intercepts (estimates of mean firing rate): 85, 78, 82, 115, and 117 spikes/s. Slope magnitudes: 0.1, 0.1, 1.6, 2.0, and 0.7 spikes $\cdot s^{-1} \cdot deg^{-1}$. Slope directions (uphill): 168, 139, 119, 121, and 40°.

During the pre-trial interval, the average firing rate of this pause-burster was ~85 spikes/s. During the fixation and visual intervals, this average firing rate was maintained, and only during the movement and reward intervals was the average firing rate substantially different from baseline. Even though there was no change in the mean firing rate during the visual interval, the firing rate of this pause-burster was modulated after target onset on some trials as can be seen by examining the tilt of the regression planes.

During the fixation interval, the planar fit was not significantly tilted. However, during the visual interval, even though the average firing rate was close to baseline, the regression plane was significantly tilted ($P < 0.001$), indicating that the firing rate of the neuron was modulated during this interval, but that, on average, the increases in firing rate on some trials were balanced by decreases in firing rate on others. During the movement and reward intervals, when the average firing rate of the neuron rose above baseline, the size of the increases in activity were still dependent on the horizontal and vertical amplitude of the movement made at the end of the trial; the planar fits for both intervals were significantly tilted ($P < 0.001$). In the visual and movement intervals, the regression planes had relatively steep tilts and were oriented so that the uphill direction was downward and contraversive. During the reward interval, the orientation of the planar fit was similar, but the tilt was not as steep.

Figure 16 plots a set of perievent time histograms that average the firing rates during 12 trials ending with contraversive and downward movements (in black) and 19 trials ending with ipsiversive and upward movements (in gray). Note that the neuron shows a marked increase in activity after contraversive target onset and a weaker decrement in response rate after ipsiversive target onset and that these modulations persisted until after movement onset. Like other SNr neurons, this pause-burster showed a large amount of trial-to-trial variance in firing rate as indicated by the large standard deviation in firing rate observed in each bin.

POPULATION ANALYSES. Figure 17*A* plots histograms of average firing rate as a percentage of baseline for all eight pause-bursters. During the fixation interval, the average firing rate of the neurons remained close to baseline. Interestingly, during the visual interval, the average firing rate was still close to the average baseline rate, even though the firing rates of most pause-bursters were modulated during this interval in opposite directions for ipsiversive and contraversive movements. However, during the movement and reward intervals, the average firing rate increased. During the fixation interval, the tilts of the regression planes were not significant for any of the eight pause-bursters. However, 75% of the regression planes were significantly tilted during the visual interval, 75% during the movement interval, and 63% during the reward interval. During the fixation interval, the regression planes (Fig. 17*B*) had relatively shallow tilts and were not consistently oriented in any direction (Rayleigh $P \cong 0.19$). In the visual and movement intervals, the regression planes were tilted much more steeply. The planes tended to be oriented so that the uphill direction was contraversive and downward although, perhaps due to the small number of pause-bursters in our sample, the slope directions did not form a significant unimodal distribution (Rayleigh $P \cong 0.14$ and 0.78 for the visual and movement intervals, respectively). Finally, during the reward interval, although the average firing rate of pause-bursters still was elevated, the firing rate of pause-bursters did not vary as strongly with the horizontal and vertical amplitude of the saccade at the end of the trial. Moreover, when there was a relationship, the orien-

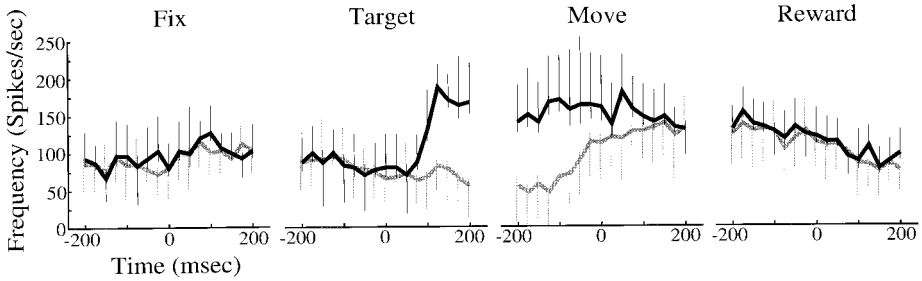

FIG. 16. Perievent time histograms for a typical pause-burster plotting the average firing rate with SD and SE during 12 trials ending with contraversive and downward (black: horizontal target position ranged from 0 to 8° right and vertical target position ranged from 6 to 16° downward) and 19 trials ending with ipsiversive and upward saccades (gray: horizontal target position ranged from 12 to 20° left and vertical target position ranged from 6 to 16° upward). Plots were constructed similarly to those in Fig. 4.

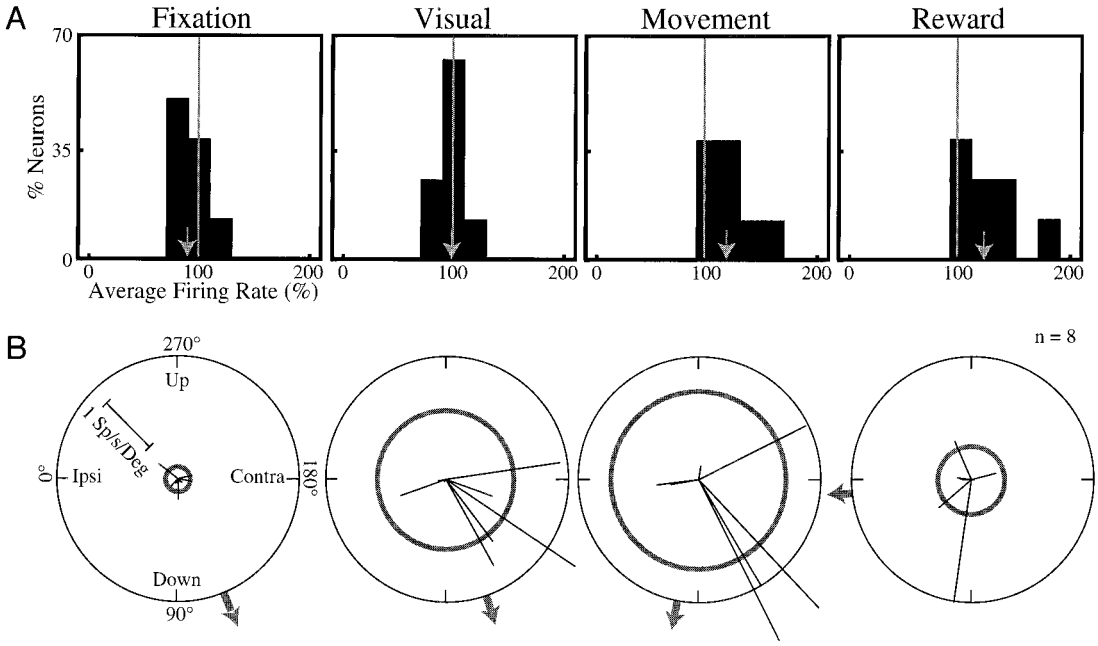

FIG. 17. Parameters from the planar fits to the response fields of 8 pause-bursters during the fixation, visual, movement, and reward intervals. Plots were constructed similarly to those in Fig. 5. *A*: histograms of planar intercepts (plotted as a percentage of baseline). Means ± SD (gray arrows): 90 ± 15, 97 ± 14, 117 ± 21, and 125 ± 27%. *B*: polar plots of planar slopes. Mean magnitudes (gray circles): 0.21 ± 0.12, 1.14 ± 0.86, 1.46 ± 1.11, and 0.56 ± 0.64 spikes · s^{-1} · deg^{-1}. Mean directions (gray arrows): 113, 110, 80, and 6°. Note that the firing rates of pause-bursters were modulated during the visual, movement, and reward intervals, and firing rates were highest during trials terminating with contraversive movements.

tation of the planar fits did not appear to be consistently biased in any particular direction (Rayleigh $P \cong 0.50$).

These population analyses indicate that the firing rates of the group of neurons we classified as pause-bursters increased after the presentation of targets for contraversive saccades and decreased after the presentation of targets for ipsiversive saccades. The increases continued until the delivery of reinforcement, while the decreases ended before the onset of the movement and were followed by increases in activity.

Histology

Figure 18 contains camera lucida reconstructions of six coronal sections from two monkeys showing the locations of 22 of the neurons included in this report. Also shown are the locations of seven additional neurons which were classified but were not studied with enough trials to be included in this report. Of these 29 neurons, 9 (2 discrete pausers, 4 universal pausers, 1 burster, and 2 pause-bursters) were recorded at the sites of electrolytic lesions. Three neurons were recorded on the same penetrations as lesions were made but at different depths. The remaining 17 neurons were recorded on electrode penetrations made at the same angle and from the same starting positions as penetrations on which lesions were made. The approximate depths of neurons in this third group were estimated by using the last thalamic somatosensory neurons encountered (presumably the ventral edge of ventroposterior thalamus) as a point of comparison between the penetration on which the lesion was made and the penetration on which the neuron of interest was recorded.

In all, 12 discrete pausers, 7 universal pausers, 6 bursters, and 4 pause-bursters were localized. All but two of these neurons were localized in the lateral portion of the SNr, just medial and ventral to the lateral geniculate nucleus (LGN) and lateral to the substantia nigra pars compacta (SNc). The anatomy of this region is shown in more detail in Fig. 19, which presents one photomicrograph from each monkey along with three SNr lesions recovered in those sections. The remaining two neurons were both identified as universal pausers and were localized above the subthalamic nucleus in the zona incerta. This indicates that neurons with the properties we describe as typical of universal pausers are distributed both inside and outside the architectural boundaries of the SNr. Whether these neurons form two functionally distinct groups based on their precise response properties cannot be concluded from our data. However, it is clear that the majority of the universal pausers we localized anatomically (5 of 7) were within the lateral SNr. It is worth noting that, although six bursters and four pause-bursters were localized to the SNr, no bursters or pause-bursters were localized to the subthalamic nucleus, suggesting that our physiological criteria for discriminating subthalamic neurons from SNr neurons were effective.

DISCUSSION

Description of the population of SNr neurons

CELL CLASSES. We recorded the activity of single SNr neurons while monkeys performed a delayed saccade task. The firing rate on each trial was measured during five intervals. For each of these five intervals, for each neuron, we constructed a response field which plotted firing rate as a function of horizontal and vertical saccade amplitude. We found that, for nearly all neurons, these response fields were planar.

From these data, we were also able to observe that the firing

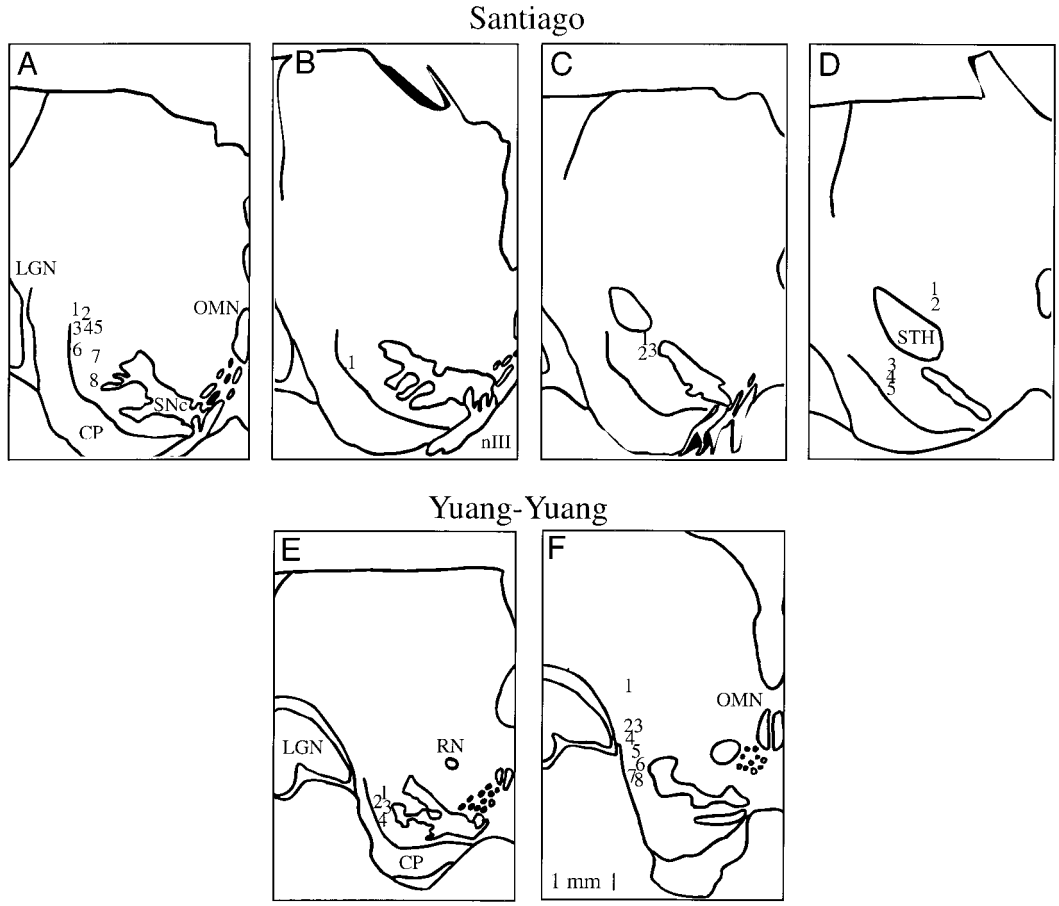

FIG. 18. Camera lucida drawings of the estimated locations of 29 identified neurons from 2 monkeys, presented in coronal section. Caudal to rostral sections are arranged from *left* to *right*. Nine neurons were located at the site of recovered electrolytic lesions (*A*, 6 and 7; *B*, 1; *C*, 2; *D*, 2; *E*, 1 and 4; *F*, 1 and 2). Three neurons were recorded on the same penetrations, but different depths, as recovered lesions (*A*, 1 and 4; *F*, 5). The remaining 17 neurons were recorded on penetrations made at the same angle and from the same starting location as recovered lesions (*A*, 2, 3, 5, and 8; *C*, 1 and 3; *D*, 1, 3, 4, and 5; *E*, 2 and 3; *F*, 3, 6, 7, and 8). We classified 12 as discrete pausers (*A*, 1, 4, and 5; *B*, 1; *C*, 1 and 3; *E*, 2; *F*, 2, 4, 5, 7, and 8), 7 as universal pausers (*A*, 2, 3, and 6; *C*, 2; *D*, 1 and 2; *F*, 1), 6 as bursters (*A*, 7 and 8; *D*, 3; *E*, 3; *F*, 3 and 6), and 4 as pause-bursters (*D*, 4 and 5; *E*, 1 and 4). Twenty-two of these neurons were included in the database described in this report; 7 neurons were not (*A*, 1, 2, 4, and 5; *F*, 3, 5, and 7). All neurons were located within the SNr (lateral to the SNc, medial to the LGN, and ventral to the CP), except for 2 universal pausers which were located in the zona incerta. CP, cerebral peduncle; LGN, lateral geniculate nucleus; nIII, oculomotor nerve; OMN, oculomotor nucleus; RN, red nucleus; SNc, substantia nigra pars compacta; STH, subthalamic nucleus.

rates of some SNr neurons decreased during the delayed saccade task but the firing rates of other SNr neurons increased. By statistically determining the intervals in which the firing rate of each SNr neuron was modulated from baseline on a significant fraction of trials and whether those modulations were increases in activity or decreases in activity, we were able to sort SNr neurons into four distinct classes.

Discrete pausers. Thirty-five percent of the neurons in our sample were classified as discrete pausers. For the modal discrete pauser, the average firing rate across all trials remained near baseline during the fixation and reward intervals but fell below baseline during the visual and movement intervals, particularly on trials in which large-amplitude contraversive saccades were produced. The response profiles of discrete pausers were relatively homogenous; the depths of the average decreases in activity and the movement directions associated with the deepest decreases were similar in most neurons. Overall, the responses of discrete pausers were qualitatively similar to the responses of many SNr neurons described by Hikosaka and Wurtz (e.g., Hikosaka and Wurtz 1983c, Fig. 7). Furthermore, like the saccade-related neurons described by Hikosaka and Wurtz, discrete pausers seemed to be distributed throughout the lateral portion of the SNr.

Universal pausers. Twenty-four percent of the neurons in our sample were classified as universal pausers. For the modal universal pauser, the average firing rate across all trials dropped further and further below baseline as trials progressed and the depth of these decreases was largely independent of the amplitude and direction of the saccade produced at the end of the trial. Our population of universal pausers was a heterogeneous class. The depth of the average decreases in firing rate varied more substantially from neuron to neuron for universal pausers than for discrete pausers. However, discrete pausers and universal pausers differed mostly in the fine temporal and spatial structures of their response fields. Thus it seems probable that, in addition to neurons similar to our discrete pausers, Hikosaka and Wurtz may have recorded from some neurons similar to our universal pausers.

Our anatomic reconstructions (Fig. 18) suggest that most, but not all, of the physiologically identified universal pausers

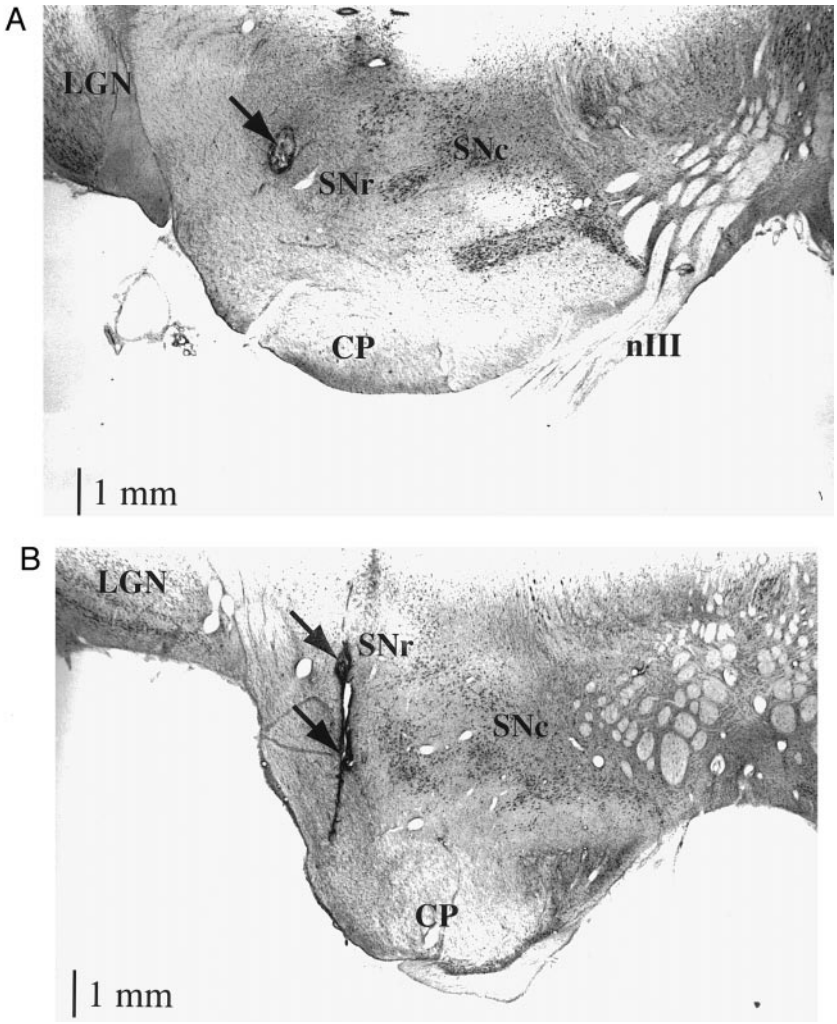

FIG. 19. Photomicrographs of the ventral portions of Fig. 18, *B* and *E*. Arrows show the locations of 3 recovered lesions in the SNr.

we encountered were located in the lateral SNr. Although most of the universal pausers we recorded from were encountered on the same penetrations, but ventral to, identifiable discrete pausers, bursters, or pause-bursters, at least two of the universal pausers we studied lay dorsal to the SNr, in the zona incerta. Oculomotor neurons in the zona incerta have been reported to fire action potentials at moderate tonic rates and to cease firing before and during both spontaneous and task-related saccades (Hikosaka and Wurtz 1983a; Ma 1996). We occasionally encountered neurons with these physiological properties during our penetrations and did not include them in our analysis because their relatively low tonic rates and responsiveness during spontaneous saccades suggested that they lay within the zona incerta. The two universal pausers histologically recovered from the zona incerta, however, had high tonic rates and were unmodulated during spontaneous saccades and thus could not be distinguished, using our physiological criteria, from the universal pausers recovered from the SNr. We have included these neurons in our analysis to highlight the fact that, when employing these physiological criteria to distinguish nigral neurons, as many as 2/7 of the universal pausers encountered and identified as nigral may, in fact, be located in the zona incerta. The universal pausers localized to the SNr appeared to be distributed throughout the lateral portion of the nucleus, although there may have been a slight tendency for these neurons to lie more dorsally than neurons from the other cell classes.

Because the firing rates of universal pausers were not strongly influenced by saccade amplitude and direction, it is possible that universal pausers carry information about some nonsaccade-related aspect of a delayed saccade trial. However, it is probable that the decreases in activity of at least some of our universal pausers were saccade-related; the perievent time histogram for our modal universal pauser (Fig. 8) demonstrated that the average firing rate of this neuron decreased abruptly before saccade onset. This temporal correlation between average firing rate and saccade onset suggests that the decrease in activity was saccade-related, although the decrease may be more tightly correlated with some other factor that was itself temporally correlated with the saccade.

Bursters. Thirty percent of the neurons in our sample were classified as bursters. For the modal burster, the average firing rate across all trials was elevated slightly above baseline during the fixation interval, further elevated during the visual and movement intervals, and maximally elevated during the reward interval. The magnitude of these increases depended on the direction and amplitude of the saccade produced at the end of the trial; the largest increases in firing rate occurred on trials terminating with large-amplitude contraversive movements. However, bursters were the most heterogeneous of our classes.

Across the population, both the magnitudes of the average saccade-related increases in activity and the movement directions associated with the largest increases varied substantially from burster to burster. In our anatomic reconstructions, we found that bursters were intermixed with discrete pausers and universal pausers in the lateral portion of the SNr.

Pause-bursters. Eleven percent of the neurons in our sample were classified as pause-bursters. For the modal pause-burster, the average firing rate across all trials remained near baseline during the fixation interval but increased above baseline during the visual, movement, and reward intervals. On any single trial, the firing rate of the modal pause-burster during the visual and movement intervals could increase or decrease depending on the horizontal and vertical amplitude of the saccade produced at the end of the trial; in general firing rates were highest during trials terminating with contraversive saccades and lowest during trials terminating with ipsiversive saccades. Neurons in the pause-burster class, which appeared to be anatomically intermixed with other SNr neurons, were homogeneous in their response properties, showing little neuron to neuron variation.

It may be important to note that the response fields of some pause-bursters were the least planar of all SNr neurons we studied. For some neurons in this class, the largest increases in activity occurred on trials terminating with small amplitude contraversive movements. It is important to note, however, that although the only neurons in our database with this type of response fields were pause-bursters, the response fields of the majority of pause-bursters more closely resembled the highly planar response fields of SNr neurons from the other three classes.

RESILIENCY AND RELIABILITY OF CELL CLASSES. For this report we sorted SNr neurons into classes by determining whether, and in which intervals, the firing rate of each neuron increased or decreased relative to baseline. We also examined other classification schemes, including a hierarchical cluster analysis, which took the relationship between firing rate and horizontal and vertical saccade amplitude into account as a classification tool. Under all the classification schemes we considered, we found that these four classes emerged with essentially the same modal characteristics as those produced by the analysis presented here. However, some neurons switched classes when we sorted our data using these different schemes. In particular, several neurons shifted between the discrete pauser and universal pauser classes or between the burster and pause-burster classes. This raises the possibility that the precise boundary between discrete pausers and universal pausers and the precise boundary between bursters and pause-bursters may not be absolute and that these two pairs of classes may actually form two continua of neuronal response properties. In general, however, we found our four basic response patterns to be a robust characterization of the SNr population.

COMPARISON OF CELL CLASSES WITH PREVIOUS REPORTS. Hikosaka and Wurtz observed that SNr neurons had high tonic firing rates (~75 spikes/s) (see Hikosaka and Wurtz 1983a, Fig. 4) punctuated by *decreases* in activity during saccadic tasks (Hikosaka and Wurtz 1983a–d). The neurons we classified as discrete pausers and universal pausers behaved in exactly this manner, showing high tonic firing rates [77 ± 19 (SD) spikes/s] and task-related decreases in activity. Unlike Hikosaka and Wurtz, we also encountered bursters and pause-bursters in the SNr that had high tonic firing rates (65 ± 23 spikes/s) and task-related *increases* in activity. Although *saccade-related* increases in the activity of SNr neurons have not been reported previously, this is consistent with the observations of physiologists who have studied SNr neurons that are responsive during skeletomuscular movement tasks. These researchers have reported that the firing rates of SNr neurons either increase or decrease from baseline in association with arm and mouth movements (DeLong and Georgopoulos 1981; Joseph and Boussaoud 1985; Joseph et al. 1985; Magarinos-Ascone et al. 1992, 1994; Schultz 1986).

Hikosaka and Wurtz observed that the firing rates of SNr neurons decreased from baseline during saccadic tasks and based partially on this observation concluded that SNr neurons influence saccade generation by disinhibiting neurons in the superior colliculus. Our observation that some SNr neurons show *increases* in rate during saccade tasks may have implications for Hikosaka and Wurtz' conclusion that the SNr influences saccades by disinhibiting neurons in the SC, although deducing the precise nature of these implications will require further investigation.

Comparison of SNr with SC and FEF

The hypothesis that the SNr participates in the generation of saccades as part of a FEF-SC circuit implies that, like collicular and frontal eye field neurons, neurons in the SNr may carry signals appropriate for specifying the metrics of upcoming saccades and/or signals appropriate for initiating saccades. Both specification and initiation signals have been examined in detail in the FEF and the SC. Our quantitative analysis of the response profiles of SNr neurons allows us to perform similar analyses of SNr spike trains and thus permits a more detailed comparison of specification and initiation-related signals in the FEF, SNr, and SC.

SIGNALS APPROPRIATE FOR SPECIFYING SACCADE METRICS. Both SC and FEF neuronal populations have been reported to carry topographically coded signals appropriate for specifying the metrics of upcoming saccades (cf. Schlag and Schlag-Rey 1990; Sparks and Mays 1983, 1990). An essential element of this code is that, in both nuclei, the firing rates of saccade-related neurons vary systematically with horizontal and vertical saccade amplitude. Like Hikosaka and Wurtz, we found that the firing rates of most SNr neurons also vary with horizontal and vertical saccade amplitude, indicating that populations of these neurons in principle could carry signals appropriate for specifying the metrics of upcoming movements. However, unlike Hikosaka and Wurtz, we found that the relationship between SNr neuronal firing rate and horizontal and vertical amplitude can be described as well by planar regressions as by Gaussian fits. Thus the SNr neurons in our sample encode horizontal and vertical saccade amplitude using either an essentially planar representation or an essentially Gaussian representation, but Gaussians centered well beyond the 40 × 40° range of amplitudes we studied. In contrast, when neurons in the FEF and SC have been studied *over a similar range of movement amplitudes and directions*, the relationships between firing rate and horizontal and vertical saccade amplitude have been observed to more closely resemble Gaussian-like functions (Bruce and Goldberg 1985; Ottes et al. 1986). This difference suggests that specification signals in the SNr are

carried in a qualitatively different form than they are in the FEF and the SC.

SIGNALS APPROPRIATE FOR INITIATING SACCADES. Both SC and FEF neurons also have been reported to carry signals appropriate for the initiation of saccades because, in both nuclei, the firing rates of saccade-related neurons have been shown to be modulated in tight temporal correlation with movement onset (cf. Hanes et al. 1995; Sparks 1978). Like Hikosaka and Wurtz, we found a temporal correlation between modulations in firing rate and saccade onset in some SNr neurons when we averaged across many trials (see Figs. 4, 8, 12, and 16). However, the high inter- and intratrial variance in firing rate made initiation-related signals, particularly initiation-related pauses, difficult for us to detect reliably on single trials using the standard thresholding-type techniques that have been applied successfully to the detection of initiation-related signals in the FEF (Hanes et al. 1995) and SC (Sparks 1978). Thus like specification signals, initiation signals seem to be carried in a qualitatively different form in the SNr than in the SC and FEF.

IMPLICATIONS FOR A POSITION OF SNr IN AN FEF-SC CIRCUIT. The diverse anatomic, physiological, and pharmacological evidence presented by Hikosaka and Wurtz are compelling arguments for a functional connection between the SNr and the SC, and our data are consistent with the hypothesis that at least some SNr neurons take part in saccade generation by disinhibiting collicular neurons. However, there is also evidence that the SNr may play a role outside of this circuit. Strick and his colleagues, for example, have used retrograde *trans*-neuronal transport of herpes simplex virus to demonstrate that the pathway from the SNr to the ventral anterior and mediodorsal thalamic nuclei (Carpenter et al. 1976; Ilinsky et al. 1985) links SNr neurons to visual area TE, area 9, area 12, and area 46 of cortex in addition to the FEF (Middleton and Strick 1996). Furthermore, Juraska and colleagues have gathered data showing that the apical dendrites of neurons in the SNc extend into the SNr, which implies that signals from the SNr may reach the pars compacta (Juraska et al. 1987). Furthermore, our physiological data indicate that the firing rates of some SNr neurons increased above baseline before some saccades in a delayed saccade task, that SNr neurons may carry information about saccadic metrics in a qualitatively different form than FEF and SC neurons, and that SNr neurons may carry information about saccadic initiation in a qualitatively different form than FEF and SC neurons. These anatomic and physiological data suggest that gating collicular discharge as part of an FEF-SC circuit may not be the only role of the SNr in the generation of saccades.

Future Directions

By developing a quantitative method for describing the spatiotemporal response profiles of SNr neurons, we were able to compare saccade-related neurons in the SNr, FEF, and SC. This same quantitative method should allow us to further explore the influence of context on SNr neurons, as originally described by Hikosaka and Wurtz (1983a–d). For example, it should be possible to quantitatively describe the response profiles of SNr neurons during both visually guided saccade tasks and memory-guided saccade tasks and to thus quantitatively assess the effect of a memory requirement on the activity of SNr neurons. A similar approach could be used to explore the effects of other forms of behavioral context on SNr activity.

In the on-going theoretical discussion of basal ganglia function, it has been suggested that the basal ganglia are activated by both goal-directed movements (cf. Kandel et al. 1991; Zigmond et al. 1999) and movements that will yield reinforcement (cf. Hollerman et al. 1998). Either explanation is consistent with Hikosaka and Wurtz' observation that SNr neurons were modulated during task-related saccades but were unmodulated during spontaneous saccades. Saccades aligning gaze with the fixation LED at the beginning of the delayed saccade task, however, are goal-directed but are not directly reinforced. By quantifying the response profile of SNr neurons during these fixational movements and comparing them to both the response profile of SNr neurons during spontaneous saccades and to the response profile of SNr neurons during saccades at the end of a delayed saccade trial, it may be possible to improve our understanding of the role of the SNr in movement generation.

We thank M. Platt, V. Ciaramitaro, M. Brown, and H. Bayer for assistance with the experiments and comments on the manuscript. We also thank J. Zhang, L. Brooks, S. Corathers, J. Mones, and H. Tamm for technical support.

This work was supported by National Eye Institute Grant EY-10536 and National Research Service Award MH11359-2 to A. Handel.

Address for reprint requests: A. Handel, Center for Neural Science, New York University, 4 Washington Place, 809, New York, NY 10003.

Received 26 March 1999; accepted in final form 29 June 1999.

REFERENCES

ALEXANDER, G. E., DELONG, M. R., AND STRICK, P. L. Parallel organization of functionally segregated circuits linking basal ganglia and cortex. *Annu. Rev. Neurosci.* 9: 357–381, 1986.

BATSCHELET, E. *Circular Statistics in Biology.* London: Academic, 1981.

BECKSTEAD, R. M., EDWARDS, S. B., AND FRANKFURTER, A. A comparison of the intranigral distribution of nigrotectal neurons labeled with horseradish peroxidase in the monkey, cat and rat. *J. Neurosci.* 1: 121–125, 1981.

BOUSSAOUD, D. AND JOSEPH, J. P. Role of the cat substantia nigra pars reticulata in eye and head movements. II. Effects of local pharmacological injections. *Exp. Brain Res.* 57: 297–304, 1985.

BRUCE, C. J. AND GOLDBERG, M. E. Primate frontal eye fields. I. Single neurons discharging before saccades. *J. Neurophysiol.* 53: 603–635, 1985.

BRUCE, C. J., GOLDBERG, M. E., BUSHNELL, M. C., AND STANTON, G. B. Primate frontal eye fields. II. Physiological and anatomical correlates of electrically evoked eye movements. *J. Neurophysiol.* 54: 714–734, 1985.

CARPENTER, M. B., NAKANO, K., AND KIM, R. Nigrothalamic projections in the monkey demonstrated by autoradiographic techniques. *J. Comp. Neurol.* 165: 401–416, 1976.

DELONG, M. R. AND GEORGOPOULOS, A. P. Motor functions of the basal ganglia. In: *Handbook of Physiology. The Nervous System. Motor Control.* Bethesda, MD: Am. Physiol. Soc., 1981, sect. 1, vol. II, part 2, p. 1017–1061.

DICHIARA, G., PORCEDDU, M. L., MORELLI, M. L., MULAS, M. L., AND GESSA, G. L. Evidence for a GABA-ergic projection from the substantia nigra to the ventromedial thalamus and to the superior colliculus of the rat. *Brain Res.* 176: 273–284, 1979.

EVARTS, E. V., KIMURA, M., WURTZ, R. H., AND HIKOSAKA, O. Behavioral correlates of activity in basal ganglia neurons. *Trends Neurosci.* 7: 447–453, 1984.

FUCHS, A. F. AND ROBINSON, D. A. A method for measuring horizontal and vertical eye movement chronically in the monkey. *J. Appl. Physiol.* 21: 1068–1070, 1966.

HANDEL, A. AND GLIMCHER, P. W. Response properties of saccade-related burst neurons in the central mesencephalic reticular formation. *J. Neurophysiol.* 78: 2164–2175, 1997.

HANES, D. P., THOMPSON, K. G., AND SCHALL, J. D. Relationship of presaccadic activity in frontal eye field and supplementary eye field to saccade initiation in macaque: Poisson spike train analysis. *Exp. Brain Res.* 103: 85–96, 1995.

HIKOSAKA, O., SAKAMOTO, M., AND NOBUO, M. Effects of caudate nucleus stimulation on substantia nigra cell activity in monkey. *Exp. Brain Res.* 95: 457–472, 1993.

HIKOSAKA, O., SAKAMOTO, M., AND USUI, S. Functional properties of monkey caudate neurons. I. Activities related to saccadic eye movements. *J. Neurophysiol.* 61: 780–798, 1989a.

HIKOSAKA, O., SAKAMOTO, M., AND USUI, S. Functional properties of monkey caudate neurons. II. Visual and auditory responses. *J. Neurophysiol.* 61: 799–813, 1989b.

HIKOSAKA, O., SAKAMOTO, M., AND USUI, S. Functional properties of monkey caudate neurons. III. Activities related to expectation of target and reward. *J. Neurophysiol.* 61: 814–832, 1989c.

HIKOSAKA, O. AND WURTZ, R. H. Visual and oculomotor functions of monkey substantia nigra pars reticulata. I. Relation of visual and auditory responses to saccades. *J. Neurophysiol.* 49: 1230–1253, 1983a.

HIKOSAKA, O. AND WURTZ, R. H. Visual and oculomotor functions of monkey substantia nigra pars reticulata. II. Visual responses related to fixation of gaze. *J. Neurophysiol.* 49: 1254–1267, 1983b.

HIKOSAKA, O. AND WURTZ, R. H. Visual and oculomotor functions of monkey substantia nigra pars reticulata. III. Memory-contingent visual and saccade responses. *J. Neurophysiol.* 49: 1268–1284, 1983c.

HIKOSAKA, O. AND WURTZ, R. H. Visual and oculomotor functions of monkey substantia nigra pars reticulata. IV. Relation of substantia nigra to superior colliculus. *J. Neurophysiol.* 49: 1285–1301, 1983d.

HIKOSAKA, O. AND WURTZ, R. H. Modification of saccadic eye movements by GABA-related substances. I. Effects of muscimol and bicuculline in the monkey superior colliculus. *J. Neurophysiol.* 53: 266–291, 1985a.

HIKOSAKA, O. AND WURTZ, R. H. Modification of saccadic eye movements by GABA-related substances. II. Effects of muscimol in monkey substantia nigra pars reticulata. *J. Neurophysiol.* 53: 292–308, 1985b.

HIKOSAKA, O. AND WURTZ, R. H. The basal ganglia. In: *The Neurobiology of Saccadic Eye Movements. Review of Oculomotor Research*, edited by R. H. Wurtz and M. E. Goldberg. New York: Elsevier, 1989, vol. 3, p. 257–281.

HOLLERMAN, J. R., TREMBLAY, L., AND SCHULTZ, W. Influence of reward expectation on behavior-related neuronal activity in primate striatum. *J. Neurophysiol.* 80: 947–963, 1998.

HOPKINS, D. A. AND NIESSEN, L. W. Substantia nigra projections to the reticular formation, superior colliculus and central gray in the rat, cat, and monkey. *Neurosci. Lett.* 2: 253–259, 1976.

HUERTA, M. F. AND HARTING, J. K. The mammalian superior colliculus: Studies of its morphology and connections. In: *The Comparative Neurology of the Optic Tectum*, edited by H. Vanegas. New York: Plenum, 1984, p. 687–773.

ILINSKY, I. A., JOUANDET, M. L., AND GOLDMAN-RAKIC, P. S. Organization of the nigrothalamocortical systems in the rhesus monkey. *J. Comp. Neurol.* 236: 315–330, 1985.

JAYARAMAN, A., BATTON, R. R., AND CARPENTER, M. B. Nigrotectal projections in the monkey: an autoradiographic study. *Brain Res.* 135: 147–152, 1977.

JOSEPH, J. P. AND BOUSSAOUD, D. Role of cat substantia nigra pars reticulata in eye and head movements. I. Neural activity. *Exp. Brain Res.* 57: 286–296, 1985.

JOSEPH, J. P, BOUSSAOUD, D., AND BIGUER, B. Activity of neurons in the cat substantia nigra pars reticulata during drinking. *Exp. Brain Res.* 60: 375–379, 1985.

JUDGE, S. J., RICHMOND, B. J., AND CHU, F. C. Implantation of magnetic search coils for measurement of eye position: an improved method. *Vision Res.* 20: 535–538, 1980.

JURASKA, J. M., WILSON, C. J., AND GROVES, P. M. The substantia nigra of the rat: a golgi study. *J. Comp. Neurol.* 172: 585–600, 1987.

KANDEL, E. R., SCHWARTZ, J. H., AND JESSEL, T. J. *Principle of Neural Science* (3rd ed.). New York: Elsevier, 1991, p. 674–675.

KUNZLE, H. AND AKERT, K. Efferent connections of cortical area 8 (frontal eye field) in *Macaca fascicularis*. A reinvestigation using the autoradiographic technique. *J. Comp. Neurol.* 173: 147–164, 1977.

LEIGH, J. R. AND ZEE, D. S. *The Neurology of Eye Movements* (2nd ed.). Philadelphia: F. A. Davis, 1991.

MA, T. P. Identification of the substantia nigra pars lateralis in the macaque using cytochrome oxidase and fiber stains. *Brain Res.* 480: 305–311, 1989.

MA, T. P. Saccade-related omnivectoral pause neurons in the primate zona incerta. *Neuroreport* 7: 2713–2716, 1996.

MAGARINOS-ASCONE, C., BUNO, W., AND GARCIA-AUSTT, E. Activity in monkey substantia nigra neurons related to a simple learned movement. *Exp. Brain Res.* 88: 283–291, 1992.

MAGARINOS-ASCONE, C., GARCIA-AUSTT, E., AND BUNO, W. Polymodal sensory and motor convergence in substantia nigra neurons of the awake monkey. *Brain Res.* 646: 299–302, 1994.

MARSDEN, C. D. The enigma of the basal ganglia and movement. *Trends Neurosci.* 3: 284–287, 1980.

MATSUMURA, M., KOJIMA, J., GARDINER, T. W., AND HIKOSAKA, O. Visual and oculomotor functions of monkey subthalamic nucleus. *J. Neurophysiol.* 67: 1615–1632, 1992.

MIDDLETON, F. A. AND STRICK, P. L. The temporal lobe is a target of output from the basal ganglia. *Proc. Natl. Acad. Sci. USA* 93: 8683–8687, 1996.

OTTES, F. P., VAN GISBERGEN, J. A., AND EGGERMONT, J. J. Visuomotor fields of the superior colliculus: a quantitative model. *Vision Res.* 26: 857–873, 1986.

PARENT, A., BOUCHARD, C., AND SMITH, Y. The striatopallidal and striatonigral projections: two distinct fiber systems in primate. *Brain Res.* 303: 385–390, 1984.

SCHLAG, J. AND SCHLAG-REY, M. Colliding saccades may reveal the secret of their marching orders. *Trends Neurosci.* 13: 410–415, 1990.

SCHULTZ, W. Activity of pars reticulata neurons of monkey substantia nigra in relation to motor, sensory, and complex events. *J. Neurophysiol.* 55: 660–677, 1986.

SEGRAVES, M. A. AND GOLDBERG, M. E. Functional properties of corticotectal neurons in the monkey's frontal eye field. *J. Neurophysiol.* 58: 1387–1419, 1987.

SOMMER, M. A. AND WURTZ, R. H. Frontal eye field neurons orthodromically activated from the superior colliculus. *J. Neurophysiol.* 80: 3331–3335, 1998.

SPARKS, D. L. Functional properties of neurons in the monkey superior colliculus: coupling of neuronal activity and saccade onset. *Brain Res.* 156: 1–16, 1978.

SPARKS, D. L. Translation of sensory signals into commands for control of saccadic eye movements: role of primate superior colliculus. *Physiol. Rev.* 66: 118–171, 1986.

SPARKS, D. L., HOLLAND, R., AND GUTHRIE, B. L. Size and distribution of movement fields in the monkey superior colliculus. *Brain Res.* 113: 21–34, 1976.

SPARKS, D. L. AND MAYS, L. E. Spatial localization of saccade targets. I. Compensation for stimulation-induced perturbations in eye position. *J. Neurophysiol.* 49: 45–63, 1983.

SPARKS, D. L. AND MAYS, L. E. Signal transformations required for the generation of saccadic eye movements. *Annu. Rev. Neurosci.* 13: 309–336, 1990.

SZABO, J. Projections from the body of the caudate nucleus in the rhesus monkey. *Exp. Neurol.* 27: 1–15, 1970.

VINCENT, S. R., HATTORI, T. AND MCGEER, E. G. The nigrotectal projection: a biochemical and ultrastructural characterization. *Brain Res.* 151: 159–164, 1978.

WILLIS, T. *The Anatomy of the Brain and Nerves (1664)*, edited by W. Feindel. Birmingham, AL: Classics of Medicine Library, 1978.

WURTZ, R. H. AND ALBANO, J. E. Visual-motor function of the primate superior colliculus. *Annu. Rev. Neurosci.* 3: 189–226, 1980.

WURTZ, R. H. AND HIKOSAKA, O. Role of the basal ganglia in the initiation of saccadic eye movements. *Prog. Brain Res.* 64: 175–190, 1986.

ZIGMOND, J. Z., BLOOM, F. E., LANDIS, S. D., ROBERTS, J. L., AND SQUIRE, L. R. *Fundamental Neuroscience*. San Diego, CA: Academic, 1999.